INVESTIGATION OF THE COMMA-HEAD STABILITY STRUCTURE OF WINTERTIME MID-LATITUDE CYCLONES USING HIGH-RESOLUTION OBSERVATIONS

BY

MELISSA KAREN PETERSON

THESIS

Submitted in partial fulfillment of the requirements
for the degree of Master of Science in Atmospheric Sciences
in the Graduate College of the
University of Illinois at Urbana-Champaign, 2012

Urbana, Illinois

Adviser:

Professor Robert Rauber

Abstract

The Profiling of Winter Storms (PLOWS) field campaign sampled twenty-four winter cyclones over the course of the 2008-2009 and 2009-2010 winter seasons. The goal of this field campaign was to investigate the distribution of instability that leads to precipitation substructures found in the comma-head (wrap-around) region of wintertime cyclones. The wrap-around region is comprised of two sectors: northern and southern. The southern sector is characterized by dry air advancing northward over the warm front. This dry air intrusion produces potential instability that is released and forms convective precipitation structures that are often observed in this region.

This study uses profiling radars and rawinsonde data to investigate the frontal and stability structure in the wrap-around region of the five winter cyclones that best sampled the interface between the dry slot air and the precipitation sector. Potential instability was found to be present in each of these cases despite being vastly different cyclones. The cyclones in this study had varying frontal structures, origins, strengths, and upper level forcing, but they all had potential instability present. Based on these analyses, the moist/dry interface on the south side of the wrap-around region of wintertime continental cyclones is characterized by deep convective cells that have heights reaching the tropopause in many cases.

The impacts of this study will lead to an increased understanding of convective snowfall. The high-resolution view of winter storms that has been provided by the remote sensing instrumentation used during PLOWS can guide

forecasters to correct their forecasts in the short-term and provide better nowcasting abilities.

Acknowledgements

First, I would like to thank my advisor, Dr. Robert Rauber, for his endless advice, patience, and encouragement throughout my Master's work. Additionally, I would like to thank the other Illinois-based PIs on the PLOWS field campaign, Dr. Greg McFarquhar and Dr. Brian Jewett for great guidance when it came to presentations and posters. I know that the success I have had here was due to you being able to bring out the best work I could produce. Another big thank you to my fellow group members. To David Plummer and Andrew Rosenow, thank you for aiding me by providing images and helping me with coding. To Jason Keeler, Michelle Pitcel, and Joe Wegman: thank you for your camaraderie and friendship and giving me great advice. I am proud to have had the opportunity to work with you all for the past three years.

Thank you to all who made the field phase of PLOWS possible: NCAR/EOL, University of Wyoming (especially Dr. David Leon), MISS team, NCAR/RAF – C130 pilots, crew, ground support, the University of Missouri, the many volunteers from Illinois, and National Science Foundation - grant AGS-0833828.

I feel I owe much of my success to the friends I have made at Illinois. The support system that I have been fortunate to find at DAS is something I will carry with me long after I am gone. I look forward to hearing about your future endeavors and the success you all deserve.

TABLE OF CONTENTS

Chapter 1: Introduction

1.1: Background

The importance and cause of convection within the comma-head region of wintertime mid-latitude cyclones has often been disputed. Very few studies have investigated continental mid-latitude cyclones and instead focus on Mid-Atlantic and Pacific Northwest wintertime cyclones. The pioneering studies, which occurred in the 1950's, used vertically pointing radars to analyze precipitation structures in the wrap-around region. Wexler and Atlas (1959) proposed that cloud-top instability, caused by lifting the dry-moist interface located where the dry slot overrides the precipitation field on the south side of the comma-head precipitation, might be responsible for the formation of potential instability that can be released to produce convective cells.

Potential instability was used to explain convection in the comma-head region until the introduction of Moist Symmetric Instability (MSI) in 1979. Many studies have been done (e.g. Wiesmueller and Zubrick 1998, Martin 1998b, Nicosia and Grumm 1999, Novak et al. 2008, 2009) to try to evaluate the validity of MSI as the mechanism for banded precipitation generation in the northwest quadrant of cyclones, but there has been limited success in attaining clear results (Wiesmueller and Zubrick 1998, Martin 1998b). This is the result of the inability to directly observe these features with existing instrumentation due to their scale, magnitude and relatively short lifetime (Novak 2008, Rauber et al 2012b).

1.2: PLOWS Field Campaign

Data from the recent Profiling of Winter Storms (PLOWS) field campaign (Rauber et al. 2012b) comes from instrumentation that has the ability to measure the characteristics of cellular convection and confirms that convection is common and is a defining characteristic of the southern edge of the wrap-around precipitation. The main goal of PLOWS is to improve the understanding of the dynamics and microphysics of heavy snowfall processes in the northwest and warm frontal quadrants of continental mid-latitude winter cyclones. PLOWS began with a two-year field campaign that occurred during the winters of 2008-2009 and 2009-2010 using instrumentation from multiple collaborating institutions. Instrumentation used during this field campaign included the Mobile Integrated Sounding System (MISS), which was provided by the National Center for Atmospheric Research (NCAR) and was comprised of a 915 MHz profiling radar and rawinsonde launch system; the Mobile Integrated Profiling System (MIPS), which was provided by the University of Alabama-Huntsville (UAH) and featured a 915 MHz profiling radar; the Mobile Alabama X-Band Radar (MAX) Doppler radar, which was provided by UAH; the University of Missouri rawinsonde launch system; and the NSF/NCAR C-130 research aircraft, featuring the Wyoming Cloud Radar (WCR), which was provided by the University of Wyoming. The instruments used in this study are the MIPS, the University of Missouri rawinsonde launch system, and the WCR.

1.3: Goals of This Study

The convection that occurs within the comma-head region of wintertime cyclones causes areas of intense snowfall that are often under-predicted. In order to provide better winter weather forecasts, there must first be an understanding of the mechanisms involved in the generation of convective snowfall. The goals of this thesis are as follows:

1. Use high-resolution profiling radars and rawinsonde data to create a stability analysis of winter cyclones, and
2. Determine if the southern end of the comma-head region is characterized by potential instability.

Chapter 2: Literature Review

2.1: The First Studies of Banded Precipitation

Pioneering studies investigating the stability structure of wintertime mid-latitude cyclones began in the 1950's, and they used vertically pointing radars to analyze precipitation structures in the wrap-around region. One of the first studies (Marshall, 1953) reported snow generation at cloud-top that merged into banded precipitation as it fell. Other studies followed [Douglas (1957), Langleben (1956), Wexler (1955), Douglas (1957), Wexler and Atlas (1959), Reed and Sanders (1953)] and observed the tendencies for convective cells to occur on the southern end of the comma head. The formation of banded precipitation was explained by the existence of potential instability in the presence of wind shear and frontogenesis in the mid-levels. Characteristics examined in these studies included horizontal extent, formation location, and vertical velocities of the convective cells.

Wexler and Atlas (1959) proposed that cloud-top instability caused by lifting the dry-moist interface could be responsible for the formation of potential instability that could be released to produce convective cells. The dry air was proposed to come from the upper troposphere/lower stratosphere (Reed, 1955). Wexler and Atlas further proposed that a lifting rate of <10 cm/s could trigger convection caused by the release of potential instability. The favored region would be the interface between the dry slot and warm front on the south side of the wrap-around region due to the differing adiabatic cooling rates of moist and dry air.

2.2: Moist Symmetric Instability/Conditional Symmetric Instability

Potential instability was used to explain the banded convective precipitation that occurs on the south end of the wrap-around region of wintertime cyclones. At the end of the 1970's, this theory lost favor after moist symmetric instability (MSI) [Bennetts and Hoskins (1979), Emanuel (1979)] was introduced. Studies predicted that vertical motions within the mesoscale convective features due to MSI in the comma head could reach speeds of 1 ms^{-1} in inviscid conditions [Emanuel (1983), Bluestein (1993)], but these speeds would be reduced to a quarter of this value when factoring in mixing and friction [Bennetts and Hoskins (1979), Persson (1995)]. All modeling studies investigating MSI generally use insufficient resolution so that they are not able to model realistic circulations of how MSI acts in the real atmosphere, and observations cannot resolve such small velocities.

Wiesmueller and Zubrick (1998) evaluated two cases in which they believed Conditional Symmetric Instability (CSI) to be present. Their study showed that banded precipitation occurred in areas where it would be expected in CSI theory, but use of this theory to aid operational forecasters is impractical due to its "cumbersome and subjective" nature (Wiesmueller and Zubrick 1998, p. 86). Martin (1998b) performed a similar study, and while the banded precipitation that formed within the model and in the actual snow event were consistent with CSI, he stated that the model resolution was too coarse to either confirm or deny CSI being responsible for the snow bands. Additionally, Nicosia and Grumm (1999) and Novak (2009) suggest that CSI may be present in the region where banded precipitation is forming, but if Conditional Instability (CI) is also present, CI will dominate, and

upright convective features will be more prevalent than the slantwise convection seen in CSI. More study will need to be done to verify MSI or CSI as the mechanism for banded precipitation in the wrap-around region of wintertime cyclones.

2.3: Observation Studies: Then vs. Now

The observational studies of the 1950's hypothesized the mechanism behind the mesoscale precipitation substructures within winter storms, but lacked high-resolution observations to confirm their hypotheses. Additionally, many studies have been conducted to evaluate the validity of MSI as the mechanism for banded precipitation generation in the northwest quadrant of cyclones; however, there has been limited success because of low resolution in both observations and modeling studies. The difficulty in obtaining quality results in both cases is due to the scale, magnitude and relatively short lifetime of the banded precipitation structures. Data from the PLOWS field campaign was attained using instrumentation that has the ability to measure the characteristics of cellular convection. Not only did the data confirm that convection is common and defining characteristic of the southern edge of the wrap-around precipitation, but updraft speeds within the southern edge of the wrap-around often greatly exceeded the 1 ms^{-1} threshold that separates MSI from potential instability.

Chapter 3: Methodology

Two goals of the PLOWS field campaign are to determine the instabilities and types of forcing that control the generation and evolution of precipitation substructures and to answer the question of how frontal scale systems above and within the boundary layer relate to precipitation substructures on the front end of the comma-head region of wintertime mid-latitude cyclones. The goals specific to this study are to use high-resolution observational data to create a stability analysis of winter cyclones and determine if the southern end of the comma-head region is characterized by potential instability.

The national composite radar image for a typical mature wintertime mid-latitude cyclone can be seen in Figure 3.1. There are two major airflows within this system that lead to the formation of the comma-head region. The first is known as the warm conveyor belt, and it is the source region for the moisture and precipitation in a mid-latitude storm that comes from the Gulf of Mexico. As this air reaches the warm front, it bifurcates, and much of the air is wrapped into the northwest quadrant of the cyclone as a rising wedge of warm, moist air. The second airflow is from the upper troposphere that descends into the central part of the cyclone. As it descends, the relative humidity drops due to adiabatic warming, and this dry air intrudes upon the southern region of the wrap-around. Where the dry air rides up over the moist air in the southern portion of the comma-head region in the northwest part of the cyclone, this area becomes critical to the creation of the cellular and convective features we see in the precipitation field. This is the area circled in red in Figure 3.1, and it is the area of investigation in this study.

This study examines five intensive operation periods (IOPs) out of the 24 that were performed during the two-year period of PLOWS. These IOPs were chosen because the deployment location of the ground instrumentation in these cases best sampled the interface between the dry-slot and wrap-around precipitation, and this is the area of investigation for this study.

The general deployment strategy for PLOWS can be seen in Figure 3.2. There were two Doppler radars: the WSR-88D and the Mobile Alabama X-band (MAX) radar supplied by the University of Alabama-Huntsville. Their proximity creates dual-Doppler lobes that enable the retrieval of horizontal winds over the rest of the ground instrumentation. Located within the dual-Doppler lobes are 915MHz vertically pointing wind profilers each co-located with a rawinsonde launch system. The first wind profiler was the National Center for Atmospheric Research (NCAR) Mobile Integrated Sounding System (MISS). This profiler was also equipped with a rawinsonde launch system. The second wind profiler is the Mobile Integrated Profiling System (MIPS) supplied by the University of Alabama-Huntsville. This was co-located with the University of Missouri sounding system. The final element to the deployment strategy was the NCAR C-130 aircraft, which was equipped with the University of Wyoming Cloud Radar (WCR), University of Wyoming Cloud Lidar (WCL), and numerous microphysical cloud probes that made in-situ measurements of the area of interest while flying between ground-based navigation beacons called vortacs.

Having the vertically pointing wind profilers co-located with a rawinsonde launch system provides a time-series of precipitation data along with

thermodynamic data, and this permits examination of the cyclone and precipitation substructures. The profilers collected data with high temporal resolution with the profiler collecting a sample from non-vertical beams every 20 seconds and a sample from the vertical beam every 40 seconds. Additionally, rawinsondes were launched every two to three hours. As these instruments were stationary during a storm, time sections of the storm passing over the site displays how the cyclone evolved with time at a point in space.

Measurements from the WCR are used to identify convective structures and determine the location of the two distinct types of precipitation: stratiform and convective. The convective precipitation was consistently seen on the southern side of the wrap-around precipitation and was characterized by cellular features. In Fig. 3.3, radar reflectivity from the LaCrosse, WI, NWS is plotted. The red dashed line represents the boundary between the stratiform and convective precipitation while the white dashed line represents the flight path of the C-130 aircraft at this time. The reflectivity data from the WCR also provides a clearer assessment of the northern extent to the dry slot air aloft, which was considerably farther north than the radar-indicated dry slot boundary based on the lower resolution WSR-88D data. Figure 3.4 is a plot of radar reflectivity from the WCR along the flight path that is shown in Fig. 3.3. Comparing Figs. 3.3 and 3.4, it is evident that the dry slot is farther north and the convective features on the south end of the wrap-around are more robust than the WSR-88D radar reflectivity image indicates.

The northernmost extent of the dry slot air aloft was identified by a combination of WCR and WSR-88D data using the WCR directly and the WSR-88D

cellular to stratiform/banded transition structure. After applying this approach using the combination of WCR and 88D images, the next step was to determine the evolution of stability at the profiler site as the storm crossed the region. Areas of potential instability are identified as regions were equivalent potential temperature with respect to ice (Θ_{ei}) decreases with height and the relative humidity with respect to ice (RH_i) is greater than or equal to 100%. To find where in the cyclone these conditions occurred based on aircraft data, a plot of the reflectivity from the WCR was overlaid with the Regional Update Cycle (RUC) model initialization of Θ_{ei} and RH_i on a flight leg perpendicular to the dry slot/precipitation interface (Fig. 3.5). The location of the warm front is easily visible as a region of tightly stacked isentropes, and the region above this is characterized by lower static stability. There are ice-saturated areas where Θ_{ei} is constant with height creating areas of neutral stability and areas where Θ_{ei} decreases with height, indicating upright potential instability. These conditions mostly conform to the convective region in the upper tropospheric dry slot region indicated by the WCR reflectivity analysis.

The cross-sections made by the C-130 w typically perpendicular to the frontal boundaries (e.g. Fig. 3.5). This was not the case for time-height sections created from the 915 MHz profiler data and rawinsondes. To identify areas of potential instability using the ground instrumentation, first, the signal to noise ratio (SNR) data from the vertical beam of the MIPS wind profiler was plotted as time vs. height. This illustrates the precipitation structures crossing the location of the profiler as the cyclone evolved. Next, a time-section of the thermodynamic data was created by plotting the rawinsonde data from the same location as time vs. height

using the RAOB (RAwinsonde OBservation) program. The soundings were launched in regular intervals to sample the cyclone as it passed overhead. By observing thermodynamic data, wind direction and speed variations in the vertical, and comparing with the WCR analyses where available, an initial analysis of frontal boundaries is performed. RUC analysis cross sections, surface and upper level maps of potential temperature and equivalent potential temperature, and horizontal wind plots were also used to aid in the frontal analysis. Frontal boundaries do not necessarily appear as sloping isentropes due to the nature of a time-section, so they can be more difficult to identify.

Once a time section of Θ_{ei} and RH_i for the location of the wind profiler was generated and a frontal analysis completed, the analysis was overlaid on the SNR and velocity plots from the wind profiler matched in time and height. Much of the air within the precipitation field of the cyclone is saturated or supersaturated with respect to ice, so this requirement of potential instability is often met.

Finally, the values of Θ_{ei} were analyzed to determine the vertical extent of the potential instability. Convection is expected to originate where Θ_{ei} first begins to decrease with height, and the depth of the layer would extend to the equilibrium level where the original Θ_{ei} at the base of the unstable layer again appears. Since observation data is being used in this study, the Θ_{ei} values were smoothed in the vertical using a 5-point smoothing algorithm to eliminate the high frequency variations in the data prior to plotting the data.

3.1 Figures for Chapter 3

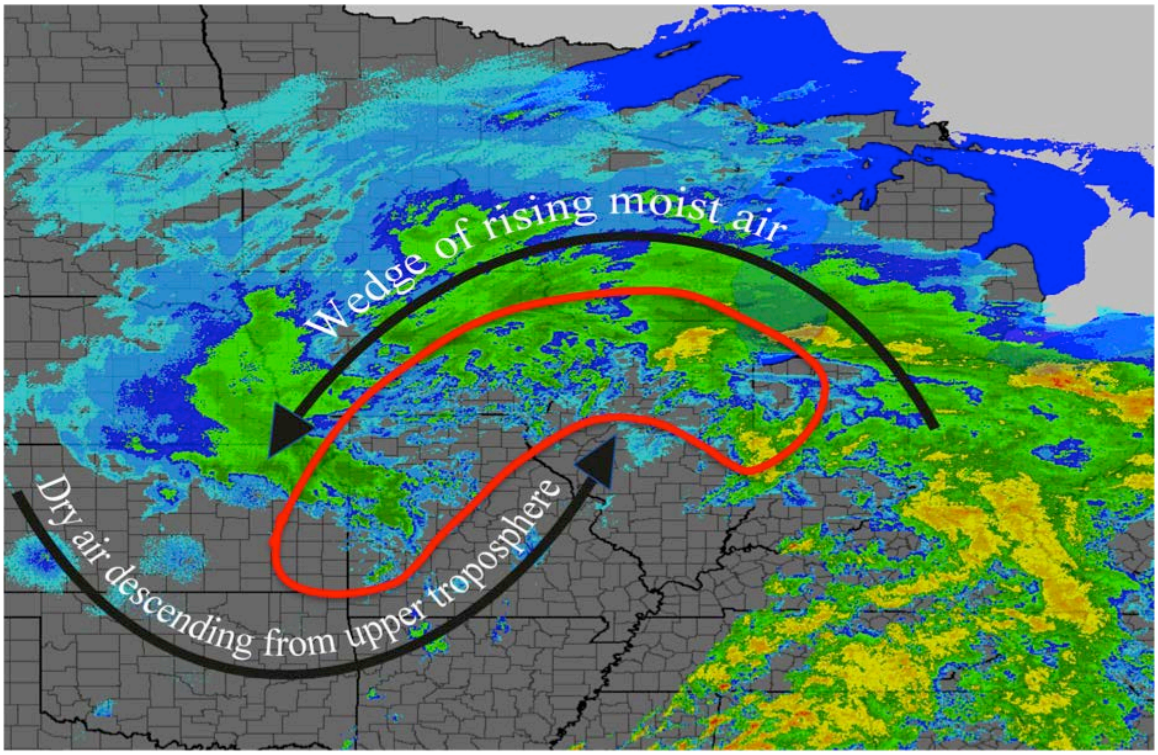

Figure 3.1. The area of investigation in this study is the cellular convection on the southern edge of the wrap-around precipitation of wintertime continental cyclones. The region outlined in red is where convective precipitation is most likely to form due to dry air originating in the upper troposphere riding over warm, moist air originating from the Gulf of Mexico.

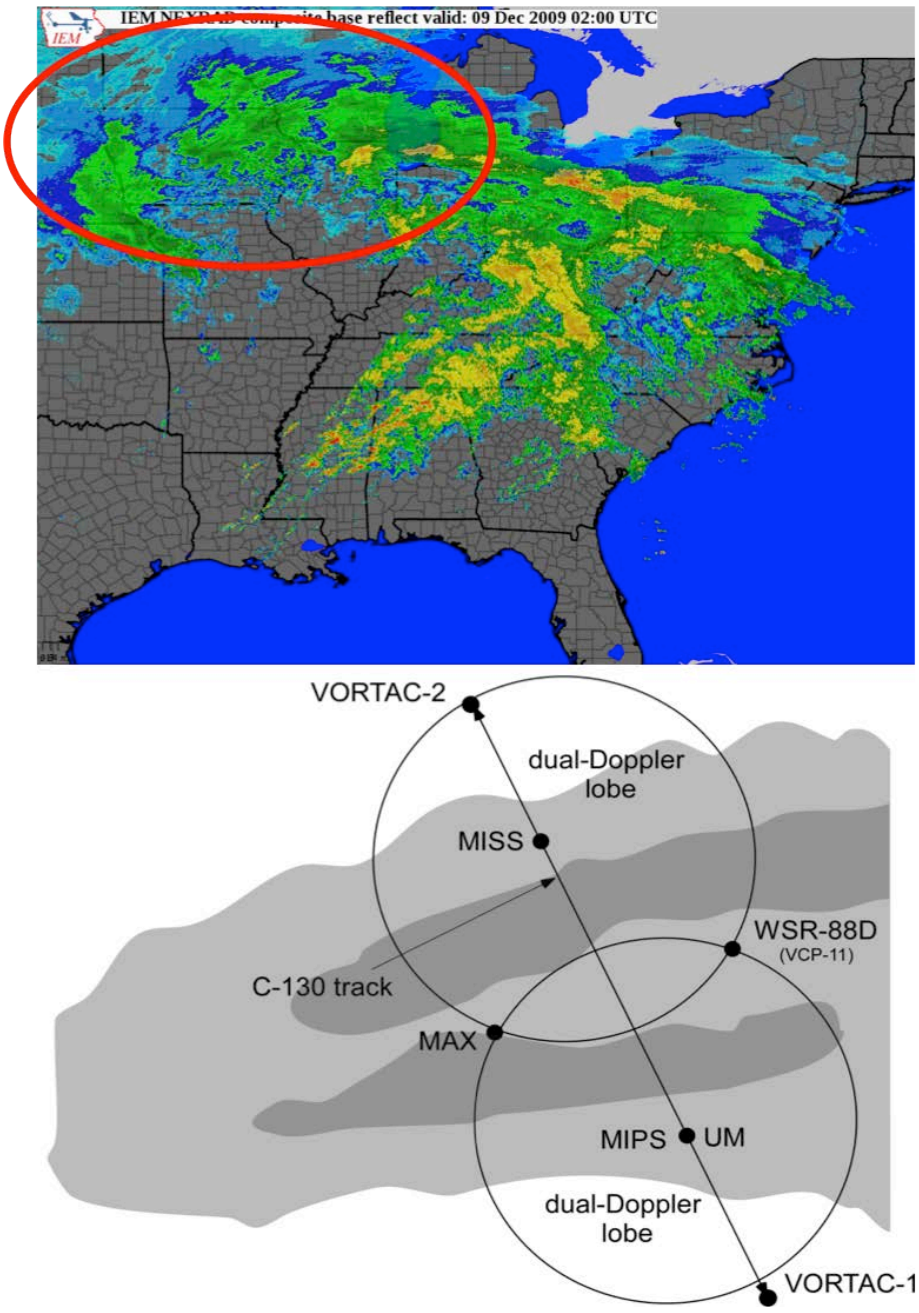

Figure 3.2. The wrap-around region is circled in red in the top image and corresponds to the gray-shaded area in the bottom image. The MAX and WSR-88D are both Doppler radars and create dual-Doppler lobes, which are regions containing sufficient data to calculate horizontal wind speed and direction. Inside of each dual-Doppler lobe is a 915 MHz wind profiler co-located with rawinsonde launch systems to provide high-resolution measurements. Finally, the C-130 aircraft flight track passes over the ground instrumentation between ground navigation beacons called vortacs.

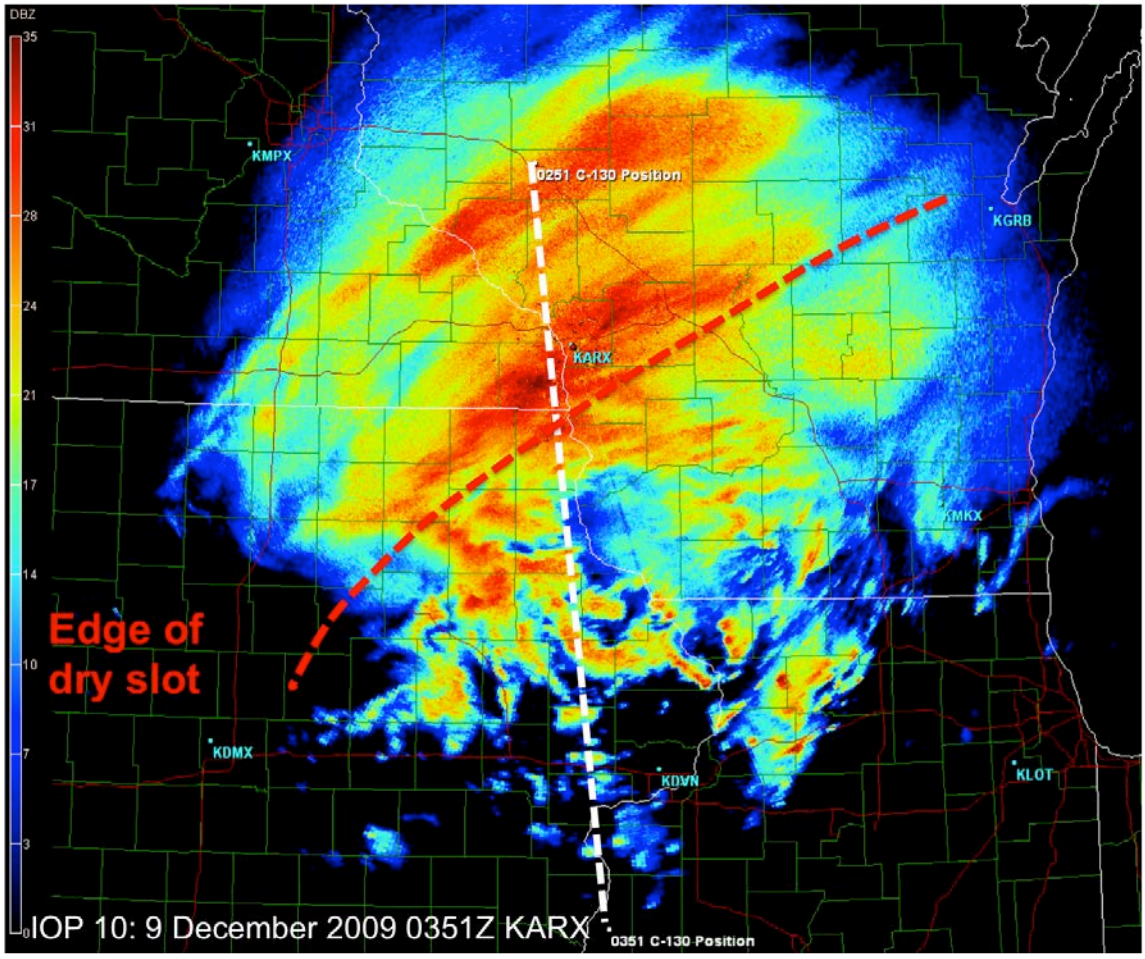

Figure 3.3. Plot of radar reflectivity from the La Crosse, WI, NWS on 9 December 2009 at 0351 UTC. The red dashed line represents the boundary between stratiform and convective precipitation as well as the northern extent of the dry slot air. The white dashed line represents the flight track for the C-130 aircraft at this time.

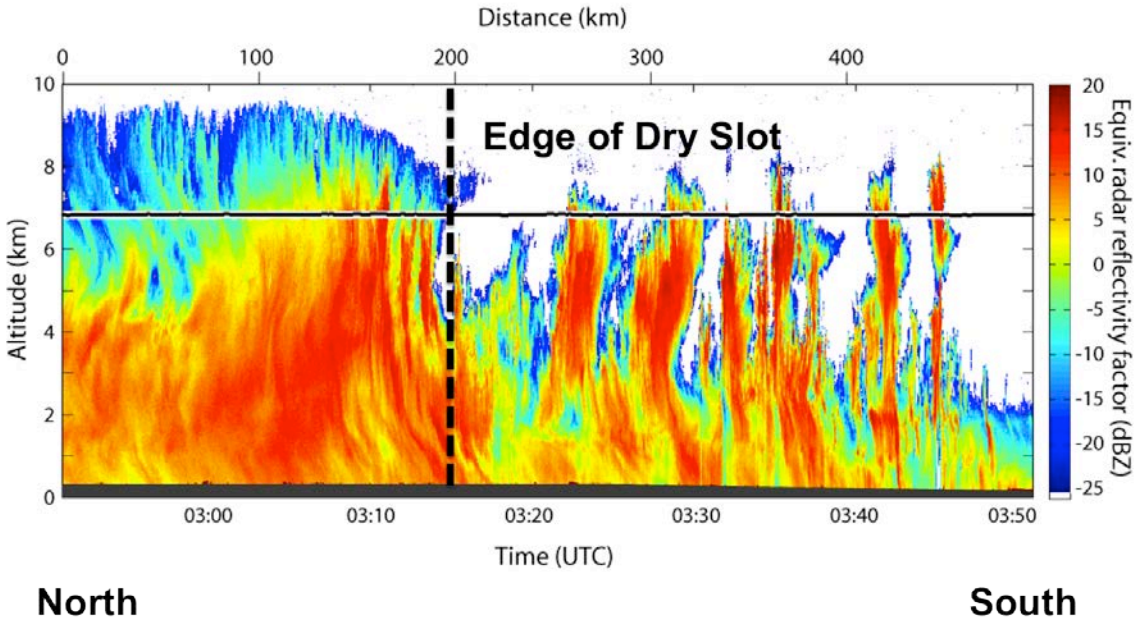

Figure 3.4. Plot of radar reflectivity from the WCR onboard the C-130 aircraft. This is the view of the cyclone along the flight path plotted on Fig. 3.3. The vertical black dashed line is in the same location as the red dashed line in Fig. 3.3 that represents the edge of the dry slot and boundary between the stratiform and convective precipitation. The convective features in the dry slot extend upwards of 8km in height.

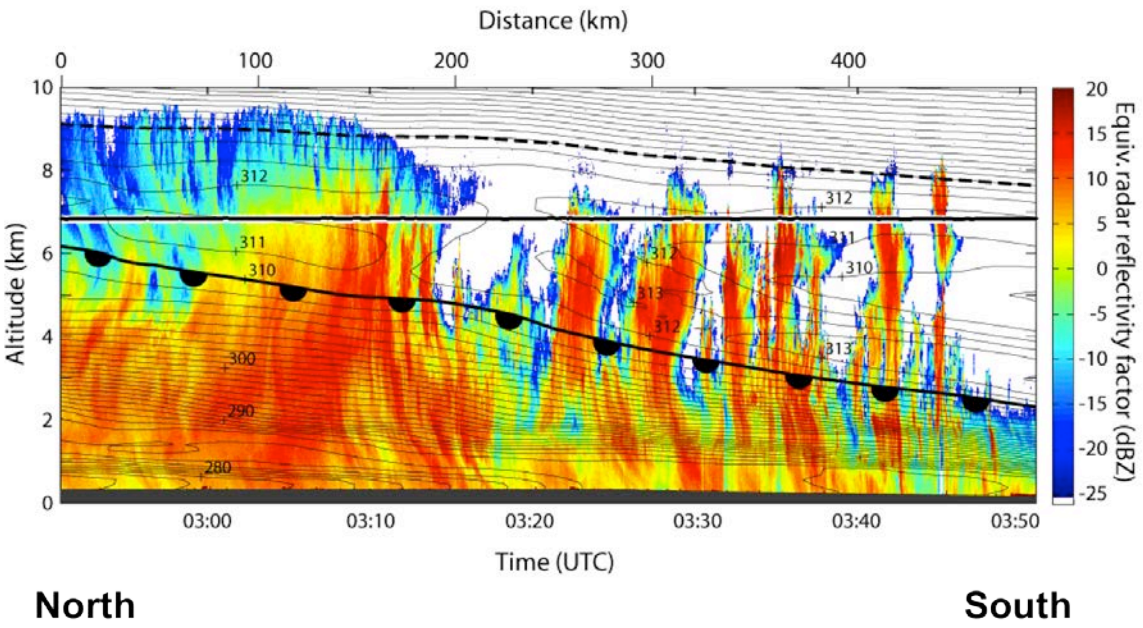

Figure 3.5. A plot of the reflectivity from the WCR overlaid with the Regional Update Cycle (RUC) model initialization of Θ_{ei} and RH_i on the flight leg shown in Fig. 3.4. The location of the warm front is easily visible as a region of tightly stacked isentropes, and the region above this is characterized by lower static stability. There are ice-saturated areas within the dry slot where Θ_{ei} decreases with height, indicating upright potential instability.

Chapter 4: Results

Five cyclones were investigated in this study, and each of these cyclones was unique in its structure, origin, and path. Despite being vastly different, each cyclone exhibited potential instability at some point in its life cycle. This is remarkable due to the location of the ground instrumentation being in a fixed location and unable to sample a large area of the cyclone. This suggests that potential instability is not a rare occurrence in a cyclone and most likely happens over the broad area of the southern edge of the wrap-around region.

4.1: IOP 1: Chicago, IL

The first cyclone investigated in this study was IOP 1. This was a Colorado Low system that passed over the Midwest from 10-12 February 2009, and the ground instrumentation was deployed near Chicago, IL. The track of the low can be seen in Fig. 4.1, and the location of the ground instrumentation relative to the evolution of the cyclone is shown in Fig. 4.2. A typical warm front and cold front characterized this cyclone, but, in addition, there was an arctic front extending north of the cyclone and trailing behind the surface cold front. This is illustrated in Fig. 4.3. Ground operations began at 0600 UTC on 11 February and ceased 0000 UTC on 12 February. Soundings were launched every two hours beginning at 1200 UTC on 11 February and concluding 0000 UTC on 12 February.

This cyclone exhibited an interesting frontal structure with a surface arctic front passing over the profiler site in the final few hours of this IOP, but there is also an upper level cold front that was under cut by the artic front. These frontal features were evident by highly compressed potential temperature contours co-located with

a shift in the wind direction seen in the rawinsonde data. After plotting the Θ_{ei} and RH_i contours on top of the wind profiler SNR, a region of potential instability can be seen beginning at 1900 UTC and continuing through to the end of the IOP. At 1900 UTC, the Θ_{ei} field begins to decrease from 317 K at 2 km to 310 K at nearly 4 km before Θ_{ei} begins to increase again, finally reaching an equilibrium level at 6km. A plot of SNR from the wind profiler, contoured Θ_{ei} and RH_i from the rawinsondes, analysis of the vertical frontal structure, and evaluation of potential instability within this cyclone is shown in Fig. 4.4.

A layer of potential instability has been positively identified, but to determine what portion of the cyclone in which it is occurring, it is compared to a national radar composite of the storm for the time of the potential instability. At 1900 UTC, the radar shows that the instability at the profiler site corresponds to the warm side of the wrap-around region, which is shown in Fig. 4.5.

4.2: IOP 8: Maxwell, IA

The second cyclone investigated in this study is the first to have occurred during the second year of the PLOWS field campaign. IOP 8 studied a weak Colorado Low system that moved very slowly over the Midwest from 23-25 November 2009, and eventually became vertically stacked as the upper level vortex became situated atop the surface cyclone. The track of the low can be seen in Fig. 4.6, and the location of the ground instrumentation relative to the evolution of the cyclone is shown in Fig. 4.7. An illustration of the horizontal frontal structure within this cyclone is shown in Fig. 4.8. Ground operations for this IOP began at 0300 UTC on 24

November and concluded at 0000 UTC on 25 November. Soundings were launched every three hours for the entirety of this IOP.

This case study was unique in that no frontal boundaries passed over the profiler site. Upper level winds were strong, over 80 kts at 6 km through the first twelve hours of the IOP, but they became calm for the rest of the IOP. This is due to the center of the upper level vortex passing over the profiler site in the latter half of this study. This upper level vortex had a cold core, and this contributed to generating much of the potential instability that is seen thought the entirety of this IOP at the profiler site. After contouring Θ_{ei}, low static stability is evident throughout the troposphere, as shown in Fig. 4.9. Potential instability starts near the ground and extends to nearly the tropopause in many regions. Values of Θ_{ei} near the surface during the beginning hours of this IOP are 312 K, decrease to 306 K at 4 km, and return to 312 K at 9 km - at the tropopause. During the latter half of the IOP, Θ_{ei} values near the surface are 306 K, decrease to 302 K near 4.5 km, and return to 306 K at 7 km – again at the tropopause.

It is difficult to accurately identify the profiler's location within this cyclone using the national composite radar reflectivity due to very weak echoes during the course of IOP 8. Surprisingly, this cyclone was ice-saturated throughout the depth of the troposphere despite not showing significant precipitation on radar reflectivity images. A tongue of dry air appears in the RH_i data above 5 km at 1800 UTC, and more intense precipitation following this feature. This is when the boundary to the dry slot and precipitation passed over the profiler site, and indeed, there is a deep layer of potentially unstable air. The dry slot/precipitation interface can be

identified on the profiler SNR plot, and potential instability is present in this location. This is doubly confirmed by identifying the location of the profiler site on the WSR-88D national composite image at 1800 UTC, which is in the southern end of the comma-head precipitation region of the cyclone, shown in Fig. 4.10.

4.3: IOP 9: Coatesville, IN

Data from IOP 9 was collected just southwest of Indianapolis, IN, in Coatesville from 2-3 December 2009. This Gulf Coast cyclone was rather robust, and, like IOP 1, featured an arctic front that passed over the profiler site. An illustration of the horizontal frontal structure within this cyclone, as well as the progression of the low, is shown in Fig. 4.11, and features an upper level front in addition to the surface warm, cold, and arctic fronts. The location of the ground instrumentation relative to the evolution of the cyclone is shown in Fig. 4.12. The ground equipment deployed perfectly for the dry slot/precipitation interface to follow along the profiler site for much of the IOP. Operations on this IOP began at 1400 UTC on 2 December and concluded just after 0600 UTC on 3 December. Soundings were launched every two hours for the entirety of this IOP excluding a missed sounding at 0400 UTC on 3 December.

Analyzing the SNR image from the profiler, convective features are evident between 0000-0200 UTC in Fig. 4.13. Between 2100 UTC and 0300 UTC, there is a region above 5 km where Θ_{ei} is decreasing or staying neutral with height up to 8.5 km. The RH_i analysis shows that much of this region is supersaturated with respect to ice, which makes this area one where the release of potential instability is possible. The vertical analysis of the frontal structure and region of possible

potential instability are indicated in Fig. 4.14. During the time period in the IOP where potential instability is possible, the profiler was located along the boundary of the wrap-around precipitation and the dry slot, which can be seen in Fig. 4.15. This is another case of potential instability being found along the southern edge of the comma-head precipitation.

4.4: IOP 10: Clinton, IA

The fourth IOP in this study is IOP 10, which occurred from 8-9 December 2009, in Clinton, IA. This Colorado Low had a very typical structure, and it was a very strong system that dropped 16+ inches of snow across southern Wisconsin. The track of the low can be seen in Fig. 4.16, and the location of the ground instrumentation relative to the evolution of the cyclone is shown in Fig. 4.17. An illustration of the horizontal frontal structure within this cyclone is shown in Fig. 4.18. Ground operations began at 0000 UTC on 8 December and continued through 1800 UTC on 9 December. Soundings were launched every three hours from 1400 UTC through 2000 UTC on 8 December and every two hours from 2000 UTC on 8 December through 0800 UTC on 9 December.

Convective features appear in the profiler SNR data starting at 2100 UTC and continue through the rest of the operational period. Evidence of potential instability in the Θ_{ei} and RH_i fields appears at 2300 UTC and continues through 0800 UTC on 9 December when sounding operations ceased. The plot of SNR, Θ_{ei} and RH_i, analysis of the vertical frontal structure, and evaluation of potential instability within this cyclone is shown in Fig. 4.19. At 2300 UTC, Θ_{ei} begins to decrease from 314 K at 4 km and returns to its equilibrium value at 8 km. At a slightly later time, 0600 UTC,

Θ_{ei} decreases from 310 K at 2.5 km and returns to its equilibrium value at 8 km. The top of the potential instability layer was consistently 8 km, and this is where the tops of the convective cells are seen on the SNR data. A look at the position of the profiler within the cyclone in Fig. 4.20 reveals that the potential instability is occurring along the southern edge of the wrap-around precipitation.

4.5: IOP 17: Franklin, IN

The final case in this study is IOP 17, which took place just south of Indianapolis, IN, in Franklin from 4-6 February 2010. This strong Gulf Low system brought heavy snowfall that crippled the Washington, DC area. The path of the low can be seen in Fig. 4.21, and the location of the ground instrumentation relative to the evolution of the cyclone is shown in Fig. 4.22. An illustration of the horizontal frontal structure within this cyclone is shown in Fig. 4.23. A unique feature of this cyclone was the secondary low in the form of a weak clipper system that mostly appeared in the mid-levels as a vorticity maximum. This feature impacted the upper level winds and made frontal analysis a challenge. Ground operations for this IOP ran from 0300 UTC on 5 February through 1600 UTC on 6 February with soundings launched every three hours from 0600 UTC on 5 February through 0600 UTC on 6 February.

Weak potential instability within this cyclone is evident starting at 1600 UTC on 5 February and continuing through to 0600 UTC on 6 February when the soundings ceased. The possible potential instability in this case is due to nearly neutral Θ_{ei} beginning at a height of 5.5 km and extending up to 8 km, illustrated in Fig. 4.24. This area wavers between being unstable with Θ_{ei} decreasing slightly with

height to becoming neutral. This region is also characterized by RH_i of 100% or greater. The profiler is located within the wrap-around region for this entire time period, and while it unusual in this study to see potential instability originating so high in the atmosphere, it can be explained by the relatively far distance the profiler was from the edge of the dry slot as shown in Fig. 4.25. Being located farther into the wrap-around precipitation of this cyclone means that the dry air overrunning the precipitation field is occurring at a higher altitude than it does near the dry slot/precipitation interface.

4.6 Results Summary

Areas where Θ_{ei} decreases with height are typically found in the latter half of the time-height cross-section. This indicates that the portion of the cyclone characterized by potential instability is the wrap-around region because it is the section of the cyclone that passed over the ground instrumentation toward the end of the IOP.

4.7 Figures for Chapter 4

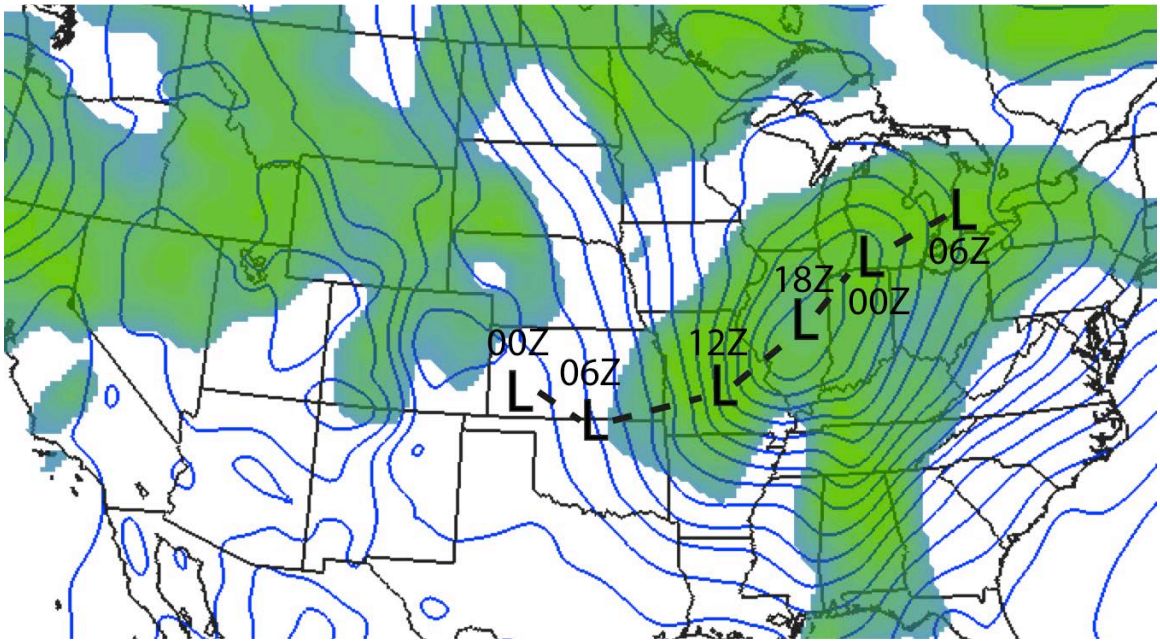

Figure 4.1. A plot of RUC 00-hr mean sea-level pressure (MSLP contoured) and 700 mb RH (greater than 50% shaded) from 11 February 2009 at 1800 UTC. The center of the cyclone investigated in IOP 1 is plotted every six hours.

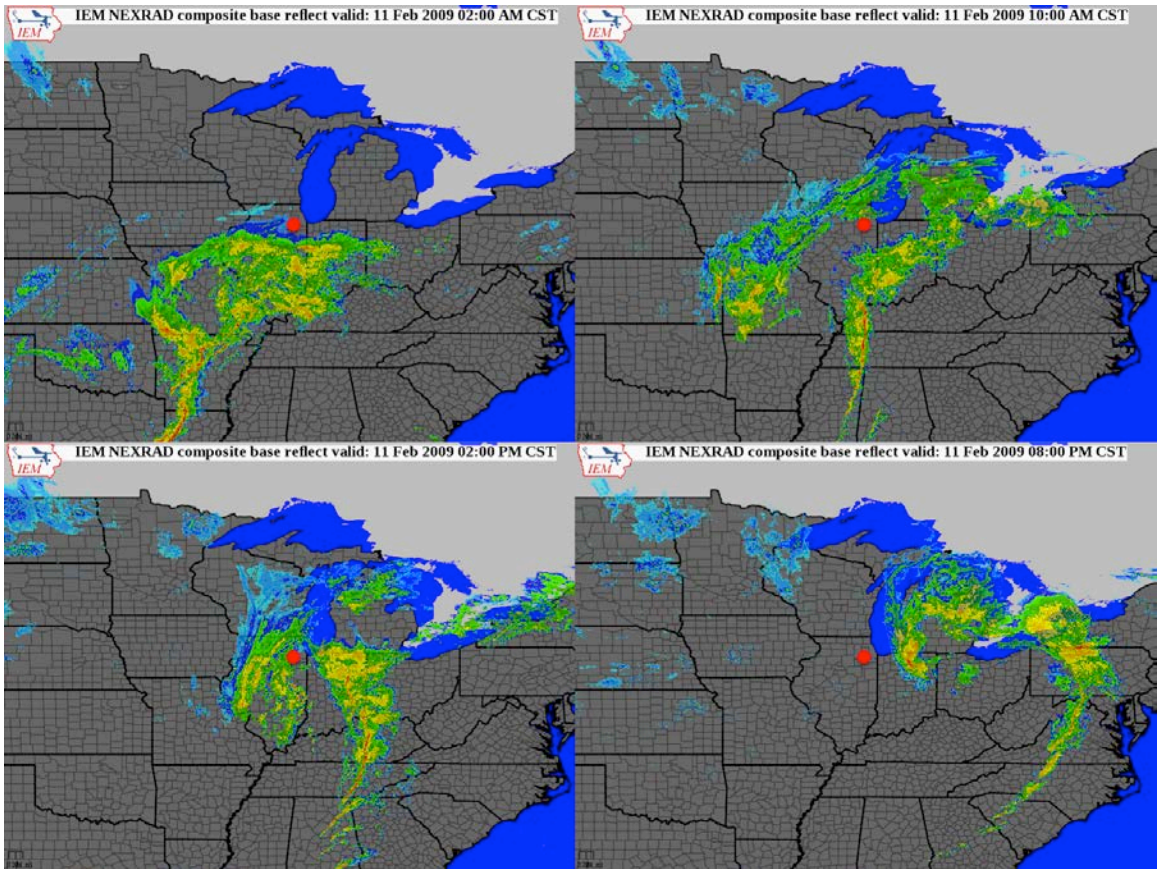

Figure 4.2. A four-panel plot of radar reflectivity demonstrating the location of the ground instrumentation (red circle) relative to the precipitation within the cyclone investigated during IOP 1. The upper left panel is from 11 February at 0800 UTC; the upper right panel is from 11 February at 1600 UTC; the lower left panel is from 11 February at 2000 UTC, and the lower right panel is from 12 February at 0200 UTC.

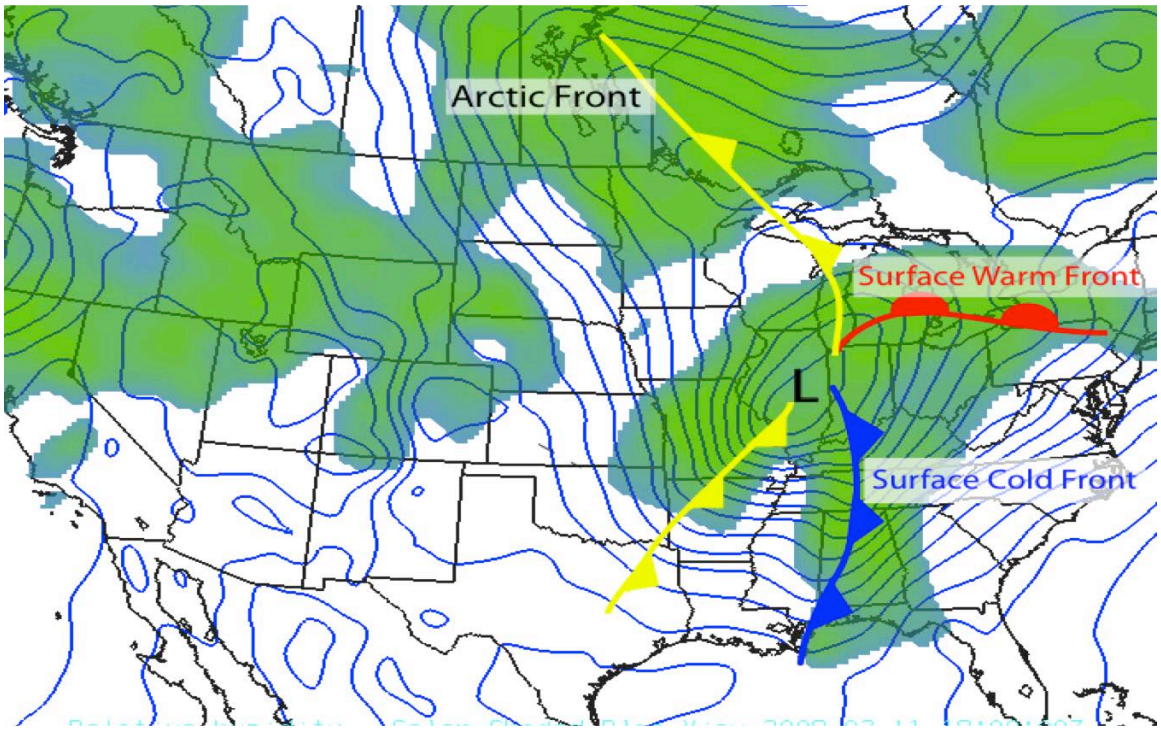

Figure 4.3. A plot the horizontal frontal features overlaid on the RUC 00-hr MSLP (contours) and 700 mb RH (shading >50%) from 11 February 2009 at 1800 UTC.

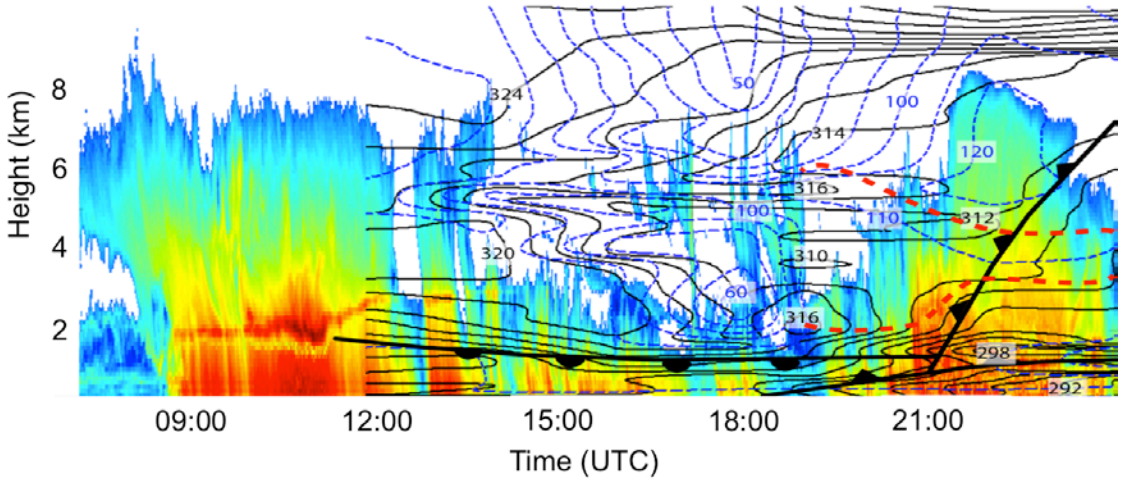

Figure 4.4. A plot of SNR, Θ_{ei} and RH_i, analysis of the vertical frontal structure, and evaluation of potential instability within this cyclone from 0600 UTC on 11 February to 0000 UTC on 12 February. The bottom red dashed line is the level where Θ_{ei} begins to decrease with height, and the top red dashed line is the level where the original Θ_{ei} at the base of the unstable layer again appears. The frontal feature that appears near the surface is the arctic front that passed over the profiler site.

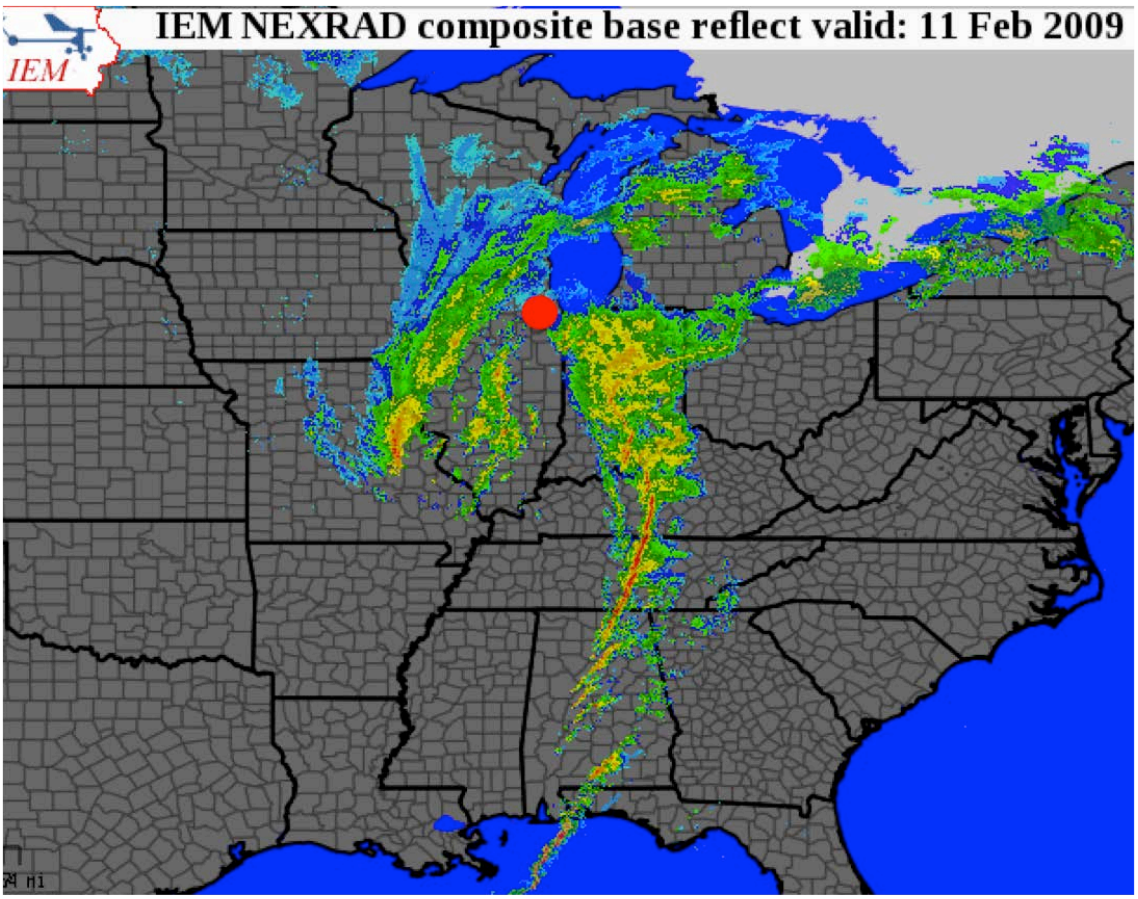

Figure 4.5. A national radar composite from 11 February 2009 at 1900 UTC. At this point in IOP 1, potential instability was indicated in the thermodynamic data, seen in Fig. 4.4. The profiler site, denoted by the red circle, is located on the south side of the comma-head region at this time.

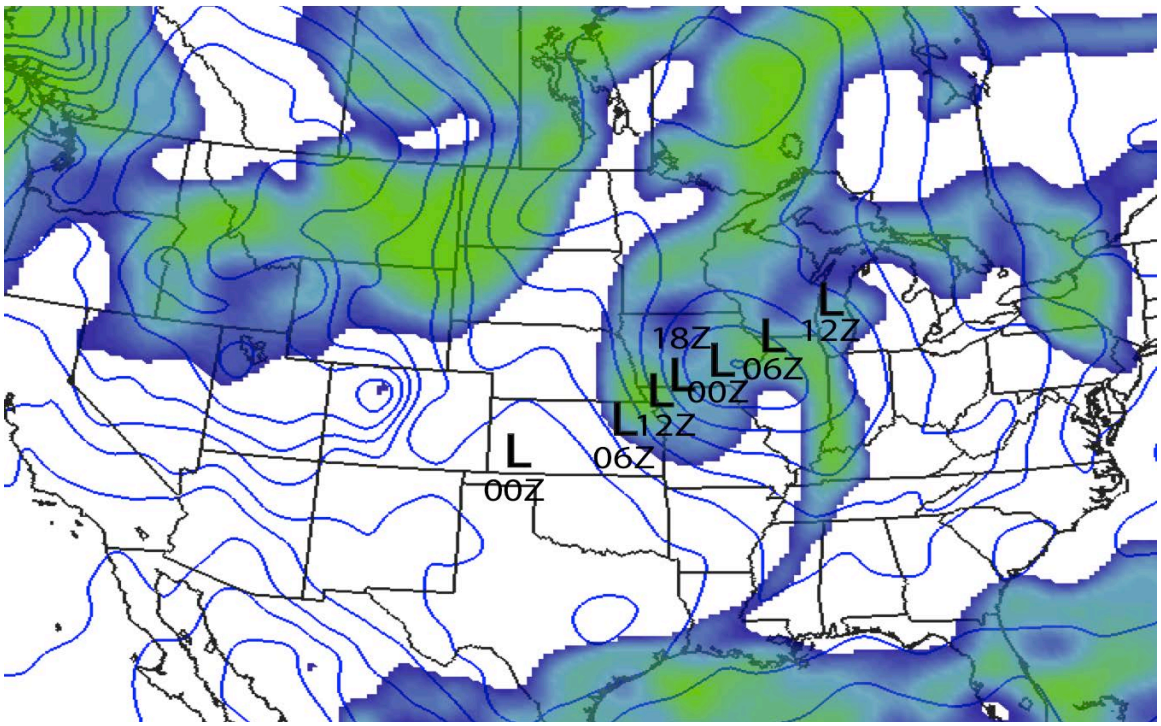

Figure 4.6. A plot of RUC 00-hr MSLP (contoured) and 700 mb RH (shaded > 50%) from 25 November 2009 at 0000 UTC. The center of the cyclone investigated in IOP 8 is plotted every six hours.

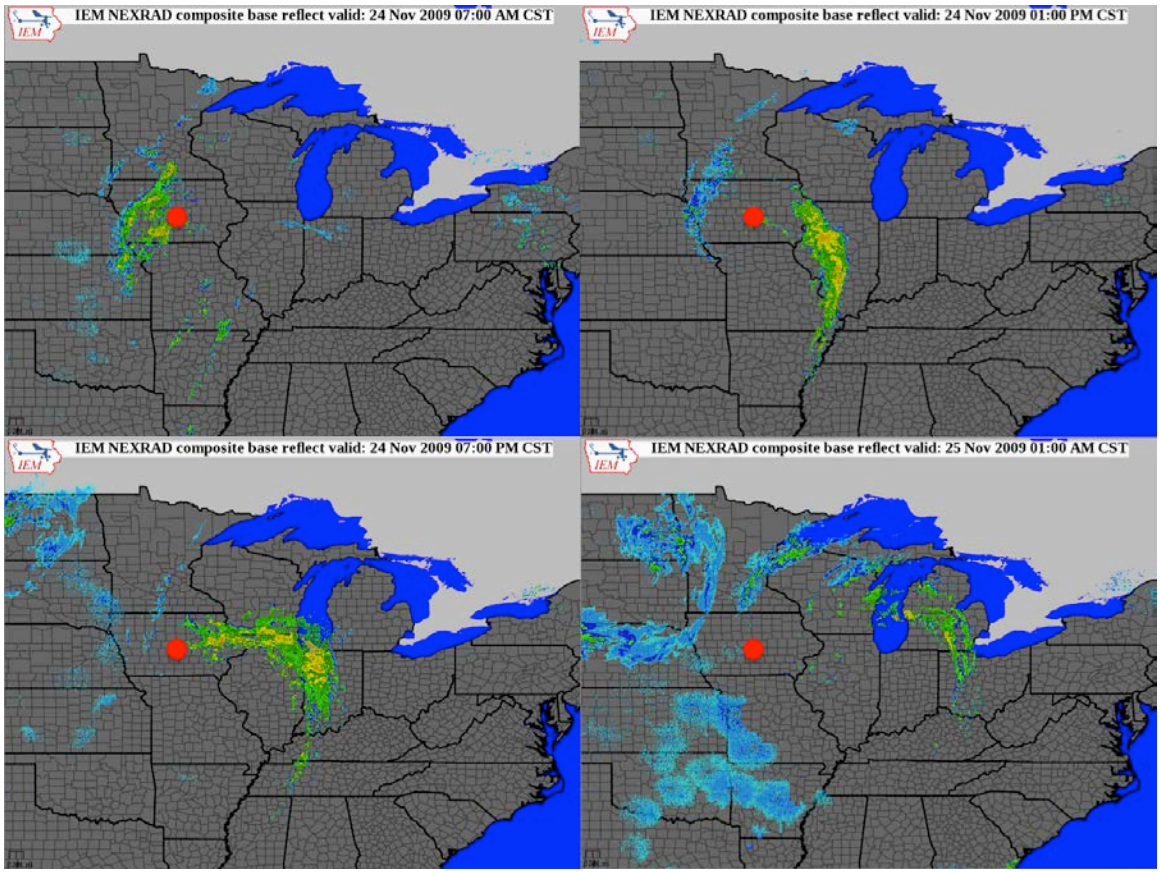

Figure 4.7. A four-panel plot of radar reflectivity demonstrating the location of the ground instrumentation (red circle) relative to the precipitation within the cyclone investigated during IOP 8. The upper left panel is from 24 November at 1300 UTC; the upper right panel is from 24 November at 1900 UTC; the lower left panel is from 25 November at 0100 UTC, and the lower right panel is from 25 November at 0700 UTC. Note how weak the precipitation appears on the WSR-88D network.

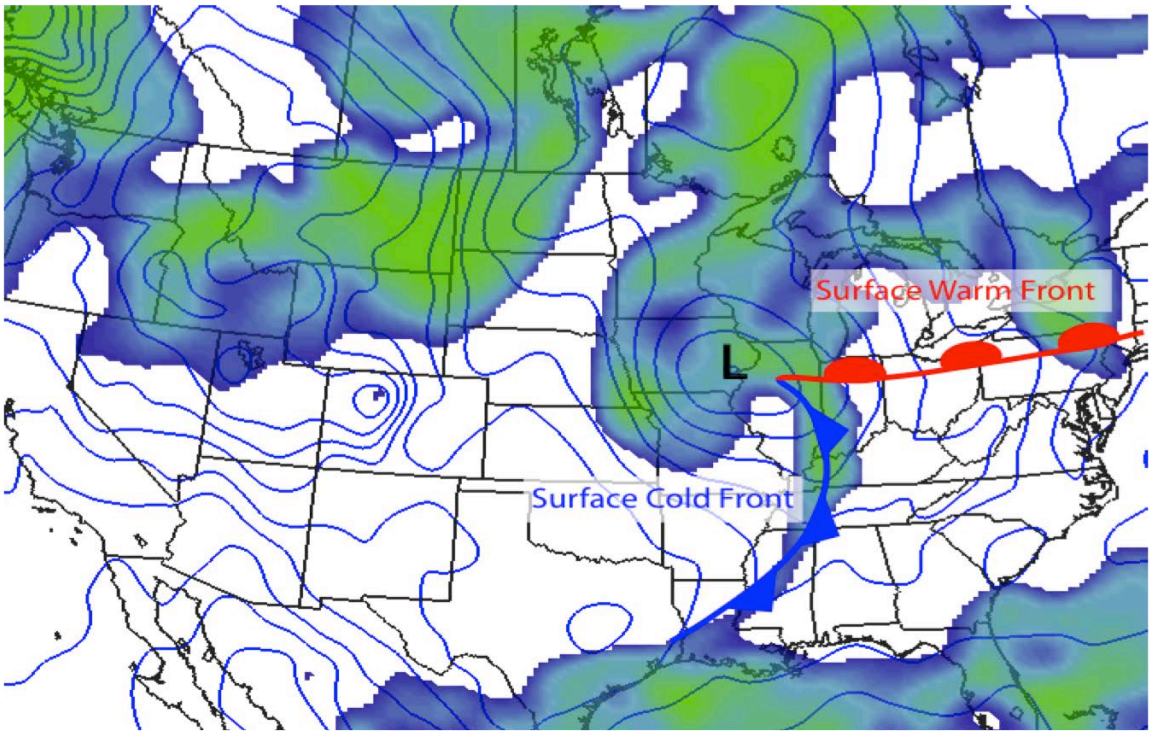

Figure 4.8. A plot the horizontal frontal features overlaid on the RUC 00-hr MSLP (contours) and 700 mb RH (shading >50%) from 25 November 2009 at 0000 UTC.

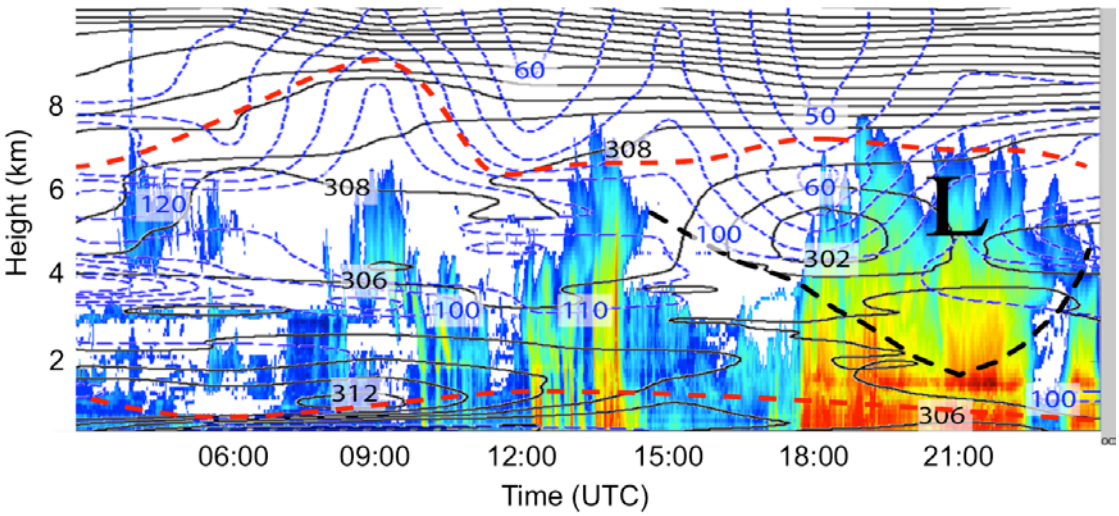

Figure 4.9. A plot of SNR, Θ_{ei} and RH_i, analysis of the vertical frontal structure, and evaluation of potential instability within this cyclone from 0300 UTC on 24 November to 0000 UTC on 25 November. The bottom red dashed line is the level where Θ_{ei} begins to decrease with height, and the top red dashed line is the level where the original Θ_{ei} at the base of the unstable layer again appears. The black dashed line represents the extent of the troposphere above the ground instrumentation that was impacted by the upper level vortex. A large portion of the troposphere was potentially unstable at the location of the ground instrumentation for the entirety of this IOP.

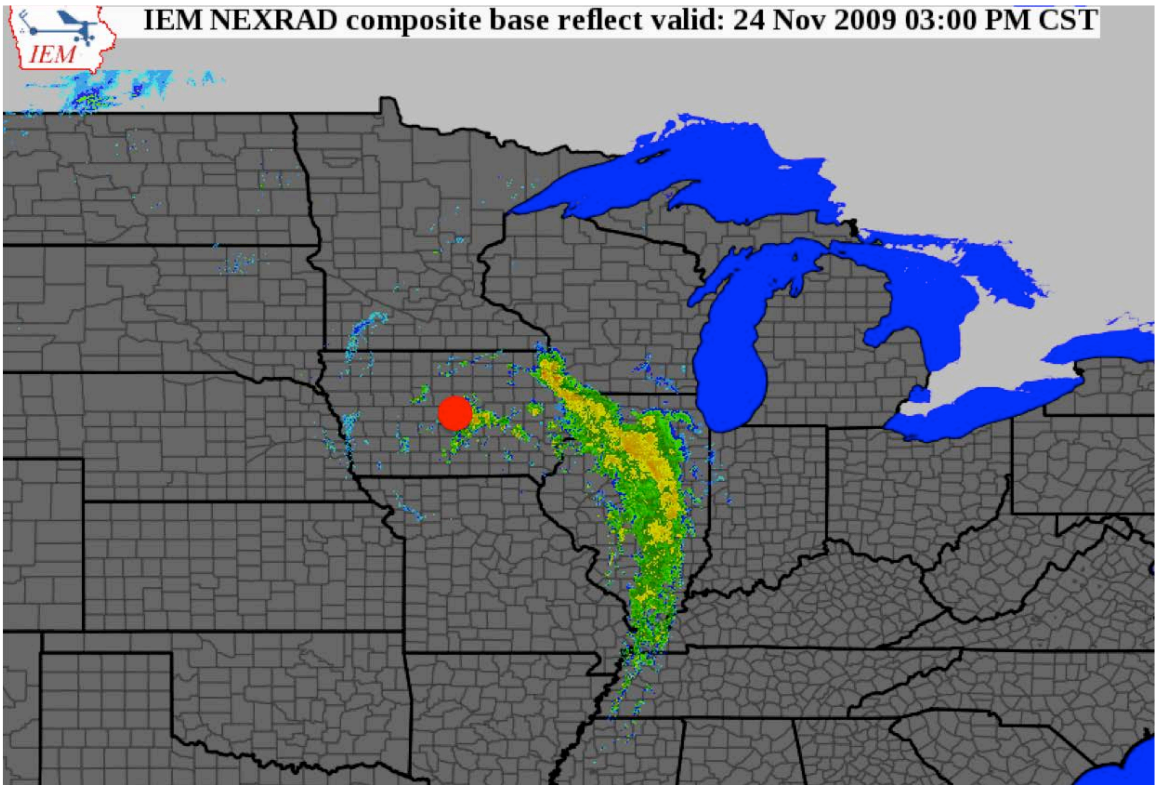

Figure 4.10. A national radar composite from 24 November 2009 at 2100 UTC. At this point in IOP 8, potential instability was indicated in the thermodynamic data in the wrap-around region, seen in Fig. 4.9. The profiler site, denoted by the red circle, is located on the south side of the comma-head region at this time.

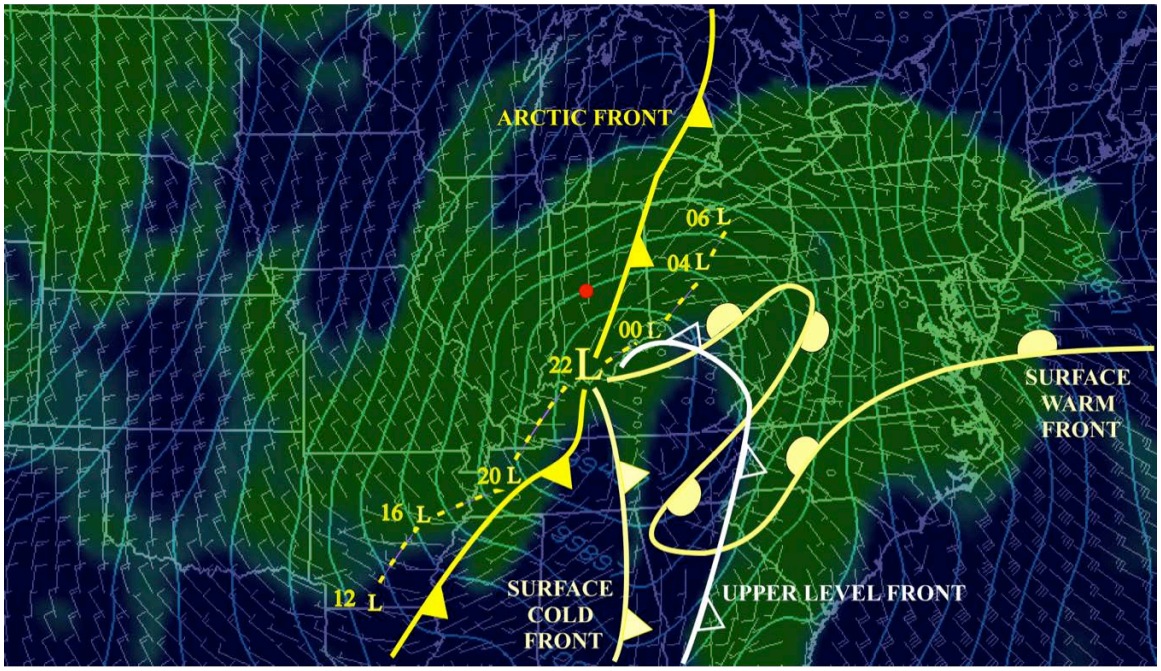

Figure 4.11. A plot of RUC 00-hr MSLP (contoured) and 700 mb RH (shaded > 50%) from 2 December 2009 at 2200 UTC. The center of the cyclone investigated in IOP 9 is plotted every four hours. Also plotted are the horizontal frontal features and the location of the ground instrumentation (red circle).

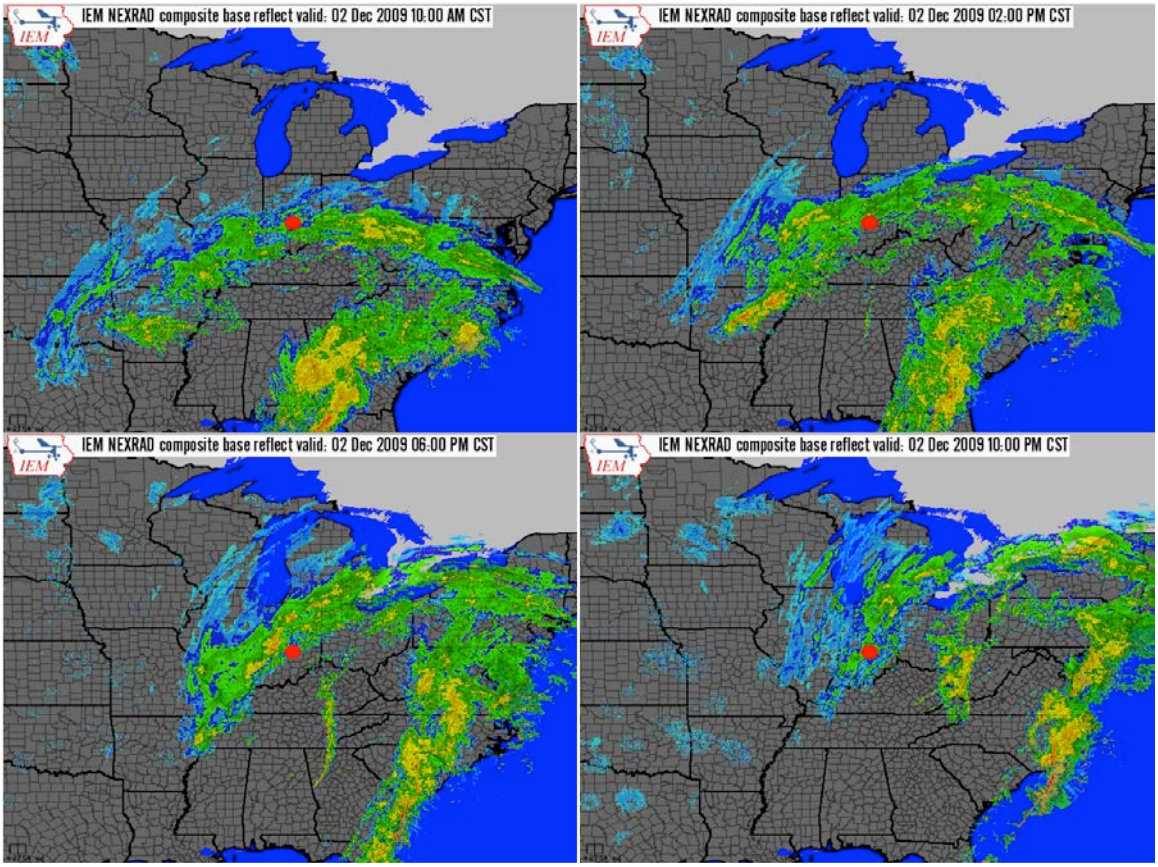

Figure 4.12. A four-panel plot of radar reflectivity demonstrating the location of the ground instrumentation (red circle) relative to the precipitation within the cyclone investigated during IOP 9. The upper left panel is from 2 December at 1600 UTC; the upper right panel is from 2 December at 2000 UTC; the lower left panel is from 3 December at 0000 UTC, and the lower right panel is from 3 December at 0400 UTC. The profiler site was situated well along the south side of the comma-head for a large portion of this IOP.

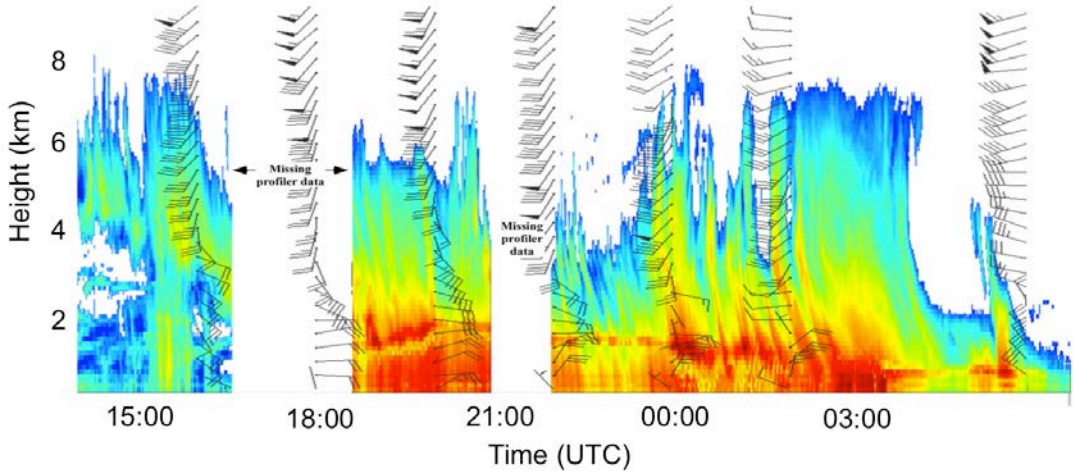

Figure 4.13. A plot of profiler SNR and winds at the time of rawinsonde launches from 1400 UTC on 2 December to 0600 UTC on 3 December. There are areas of missing profiler data when the profiler was not functioning properly. Convective features become apparent at 0000 UTC.

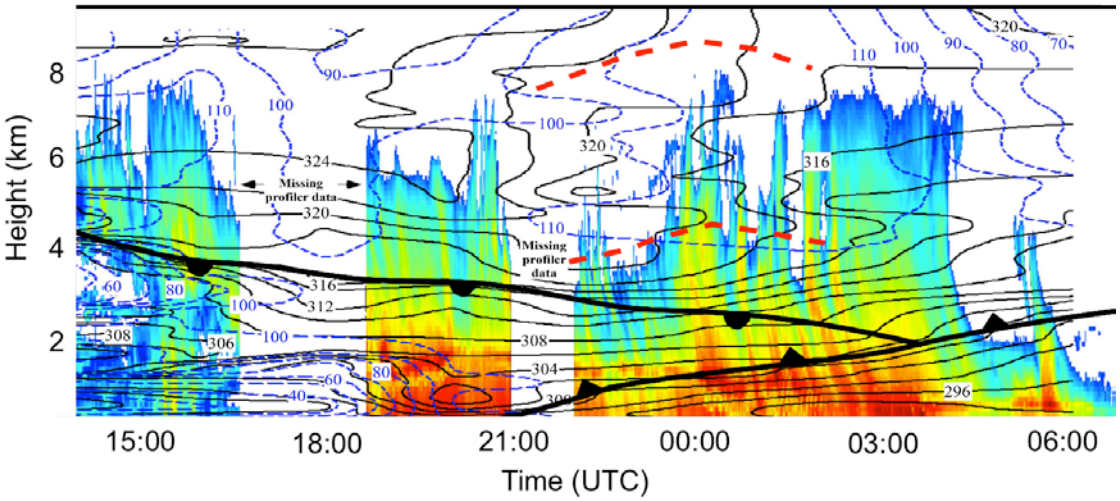

Figure 4.14. A plot of SNR, Θ_{ei} and RH_i, analysis of the vertical frontal structure, and evaluation of potential instability within this cyclone from 1400 UTC on 2 December to 0600 UTC on 3 December. The bottom red dashed line is the level where Θ_{ei} begins to decrease with height, and the top red dashed line is the level where the original Θ_{ei} at the base of the unstable layer again appears. The frontal features that passed over the ground instrumentation are a warm front, which was undercut by the cold front as the wrap-around region reached the profiler site.

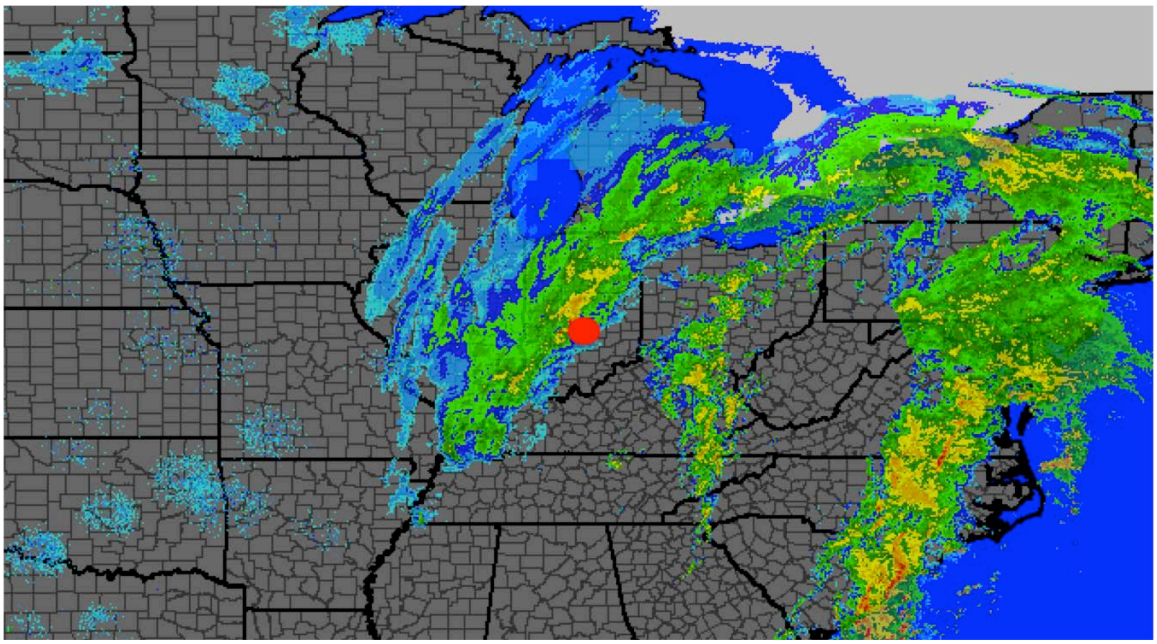

Figure 4.15. A national radar composite from 3 December 2009 at 0200 UTC. At this point in IOP 9, potential instability was indicated in the thermodynamic data in the wrap-around region, seen in Fig. 4.14. The profiler site, denoted by the red circle, is located on the south side of the comma-head region at this time.

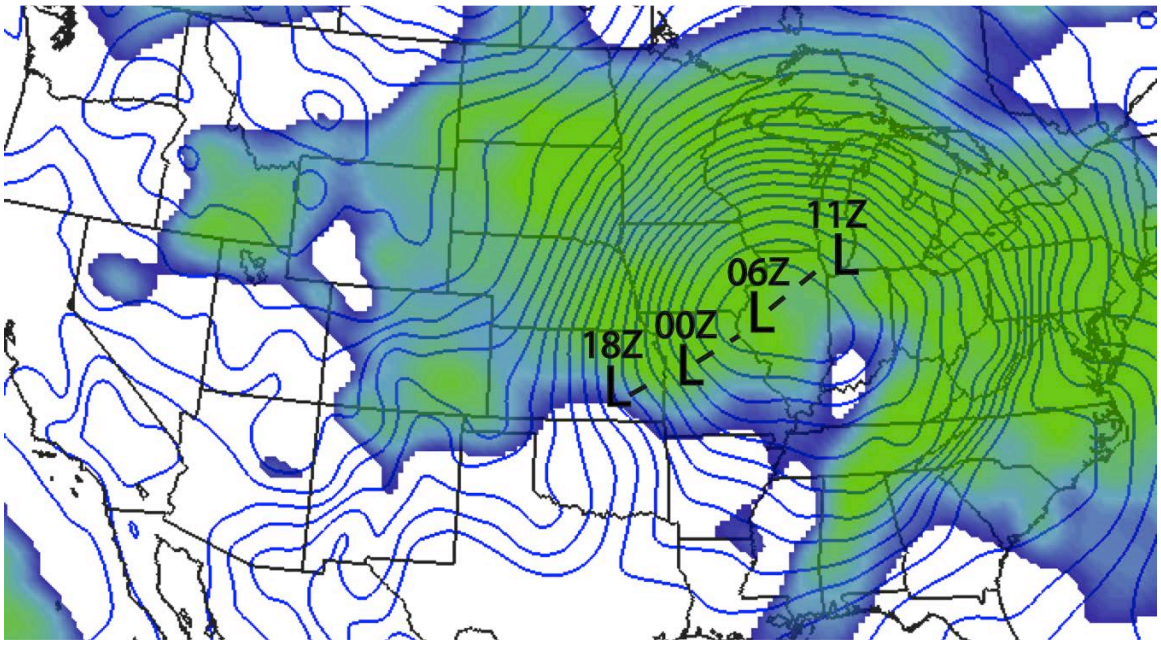

Figure 4.16. A plot of RUC 00-hr MSLP (contoured) and 700 mb RH (shaded > 50%) from 9 December 2009 0600 UTC. The center of the cyclone investigated in IOP 10 is plotted for various times during this IOP as it progressed through the Midwest.

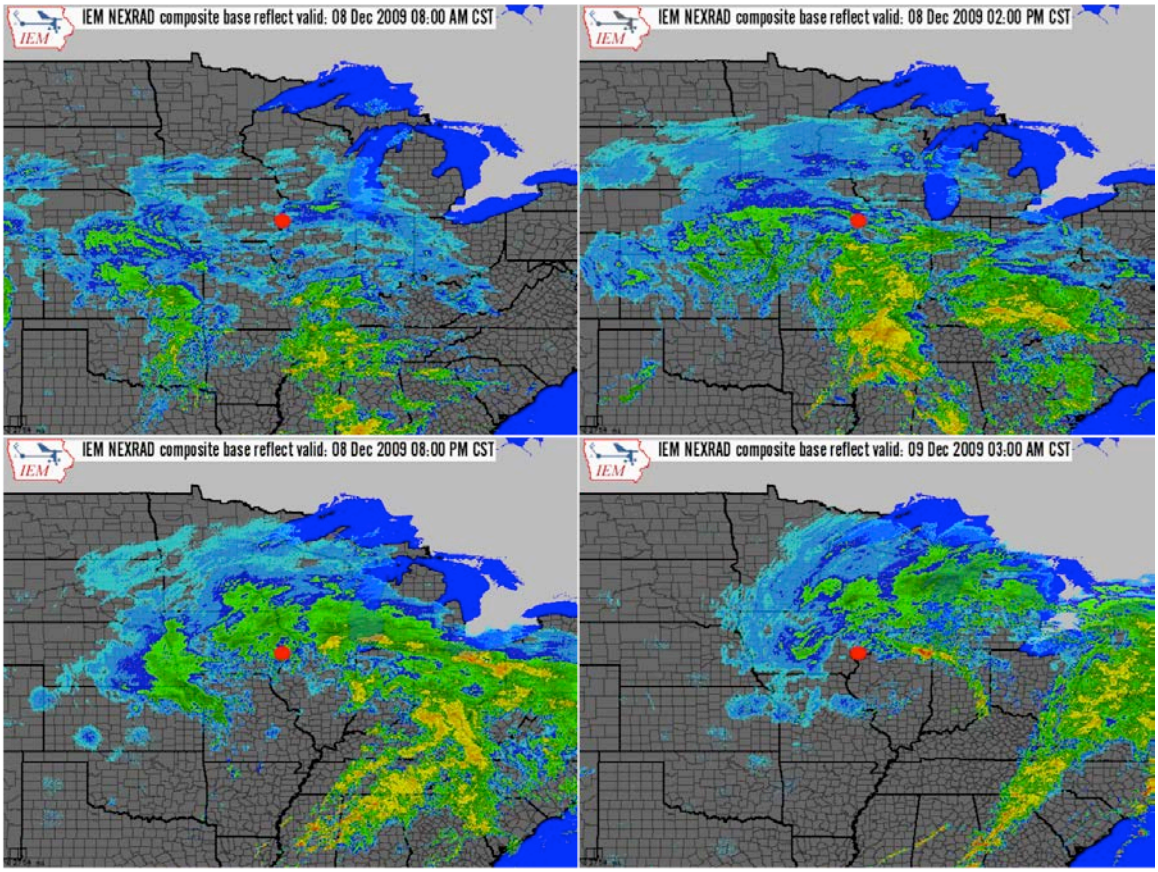

Figure 4.17. A four-panel plot of radar reflectivity demonstrating the location of the ground instrumentation (red circle) relative to the precipitation within the cyclone investigated during IOP 10. The upper left panel is from 8 December at 1400 UTC; the upper right panel is from 8 December at 2000 UTC; the lower left panel is from 9 December at 0200 UTC, and the lower right panel is from 9 December at 0900 UTC.

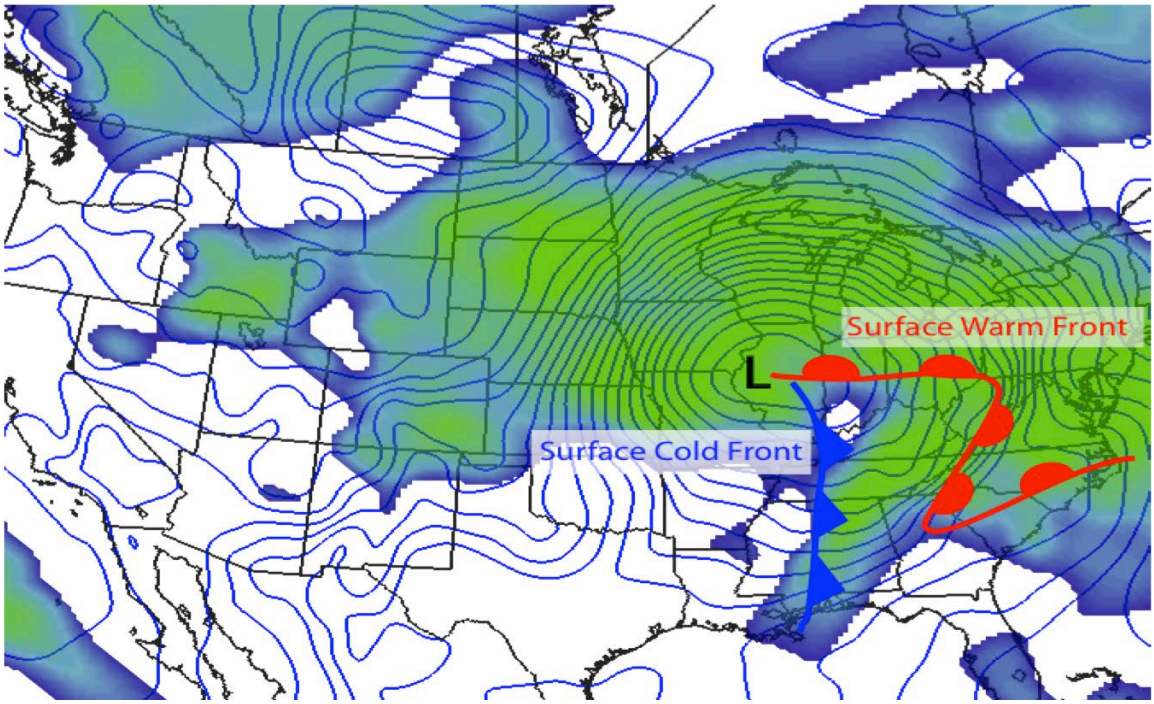

Figure 4.18. A plot the horizontal frontal features overlaid on the RUC 00-hr MSLP (contours) and 700 mb RH (shading >50%) from 9 December 2009 at 0600 UTC.

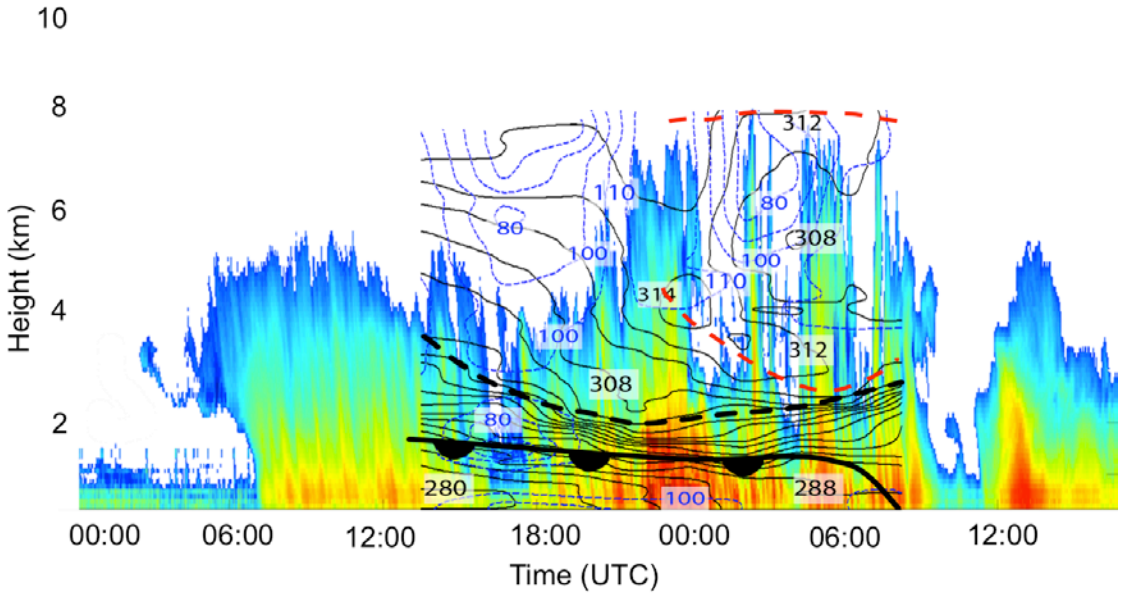

Figure 4.19. A plot of SNR, Θ_{ei} and RH_i, analysis of the vertical frontal structure, and evaluation of potential instability within this cyclone from 0000 UTC on 8 December to 1800 UTC on 9 December. The bottom red dashed line is the level where Θ_{ei} begins to decrease with height, and the top red dashed line is the level where the original Θ_{ei} at the base of the unstable layer again appears. The warm front passed over the profiler site as well as a moisture boundary indicated by the black dashed line.

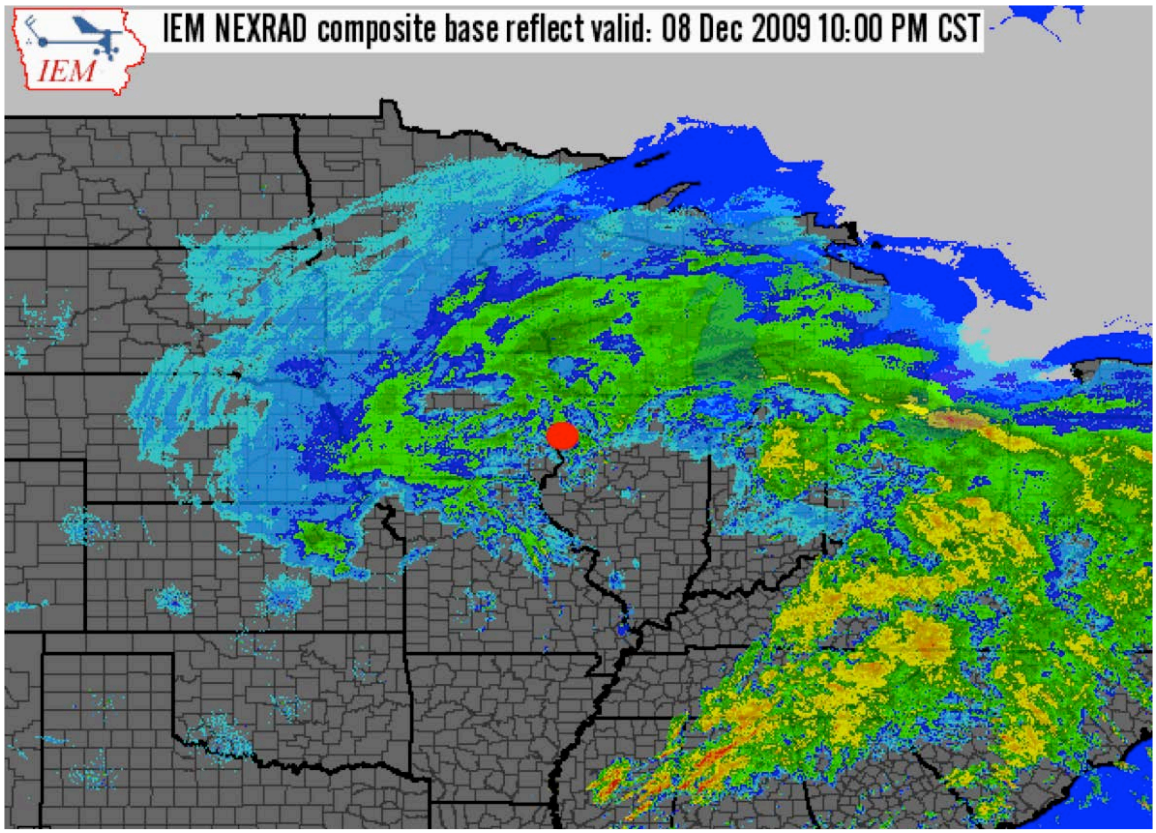

Figure 4.20. A national radar composite from 9 December 2009 at 0400 UTC. At this point in IOP 10, potential instability was indicated in the thermodynamic data in the wrap-around region, seen in Fig. 4.19. The profiler site, denoted by the red circle, is located on the south side of the comma-head region at this time.

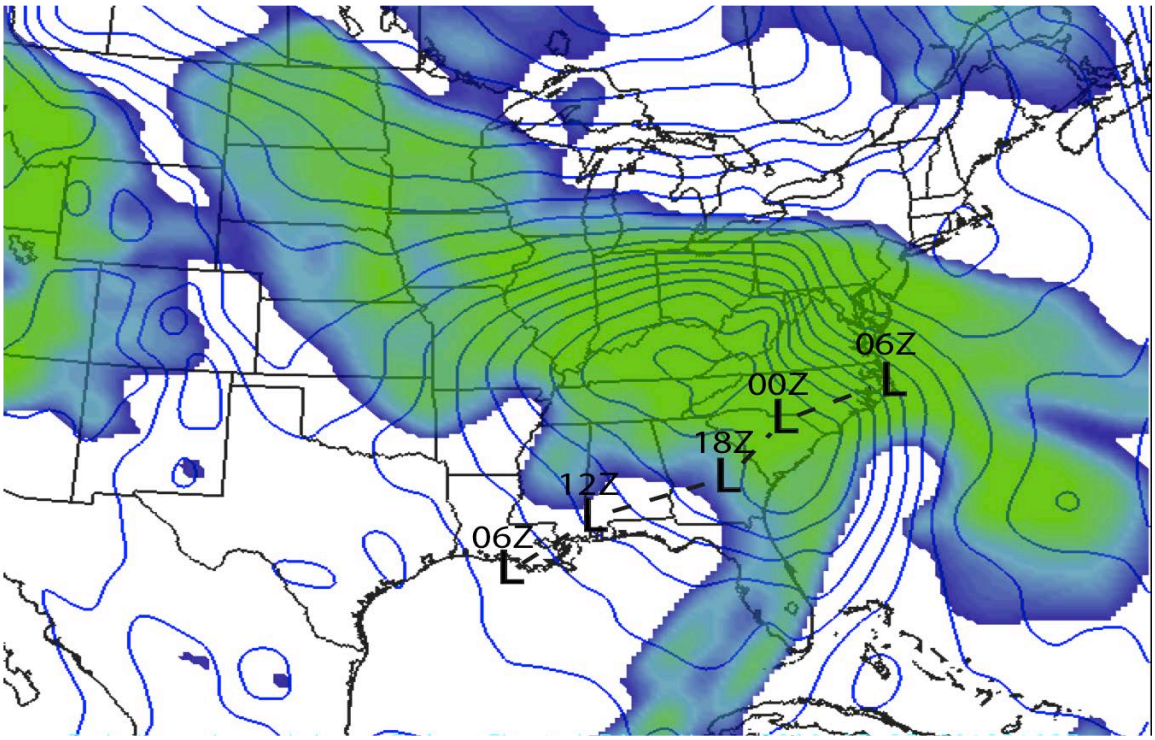

Figure 4.21. A plot of RUC 00-hr MSLP (contoured) and 700mb RH (shaded > 50%) from 6 February 2010 at 0000 UTC. The center of the cyclone e investigated in IOP 17 is plotted every six hours.

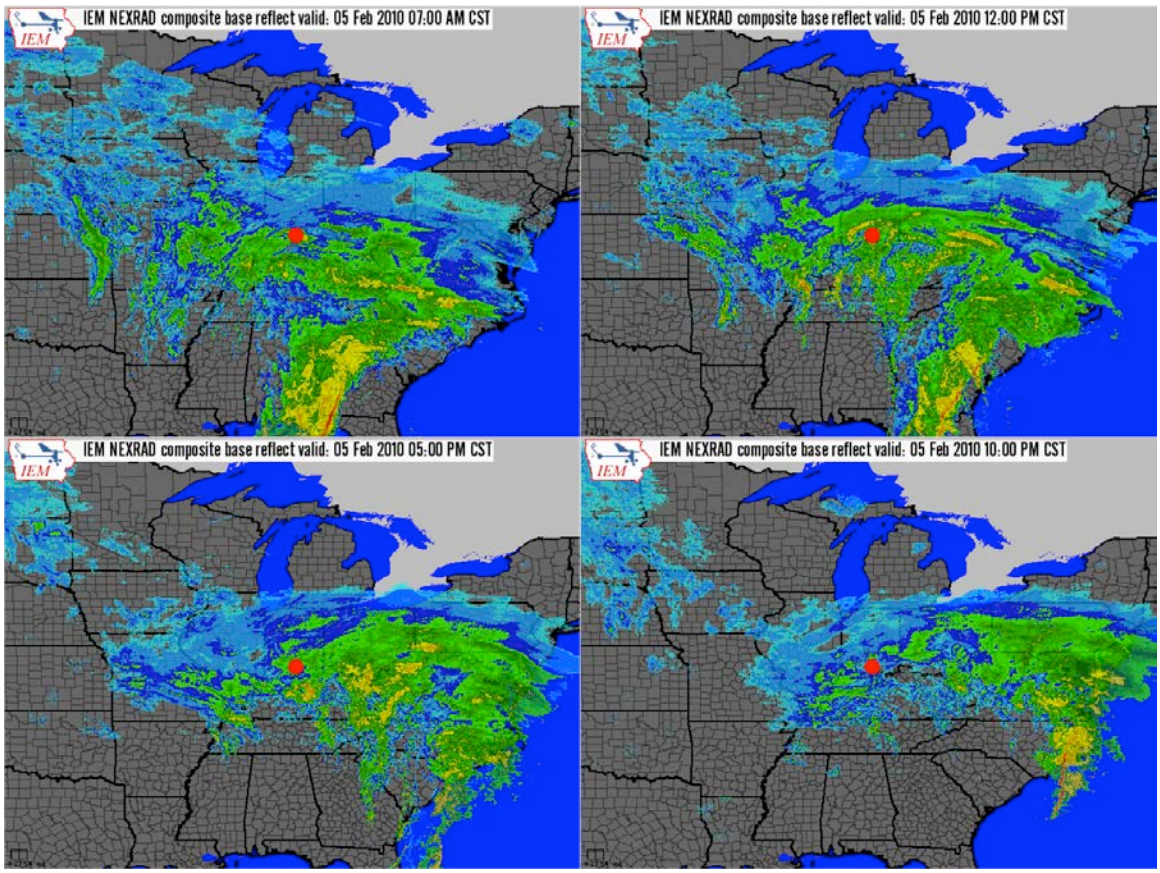

Figure 4.22. A four-panel plot of radar reflectivity demonstrating the location of the ground instrumentation (red circle) relative to the precipitation within the cyclone investigated during IOP 17. The upper left panel is from 5 February at 1300 UTC; the upper right panel is from 5 February at 1800 UTC; the lower left panel is from 5 February at 2300 UTC, and the lower right panel is from 6 February at 0400 UTC. The ground instrumentation was stationed farther from the dry slot/precipitation interface in this IOP compared to the ones previously examined in this study.

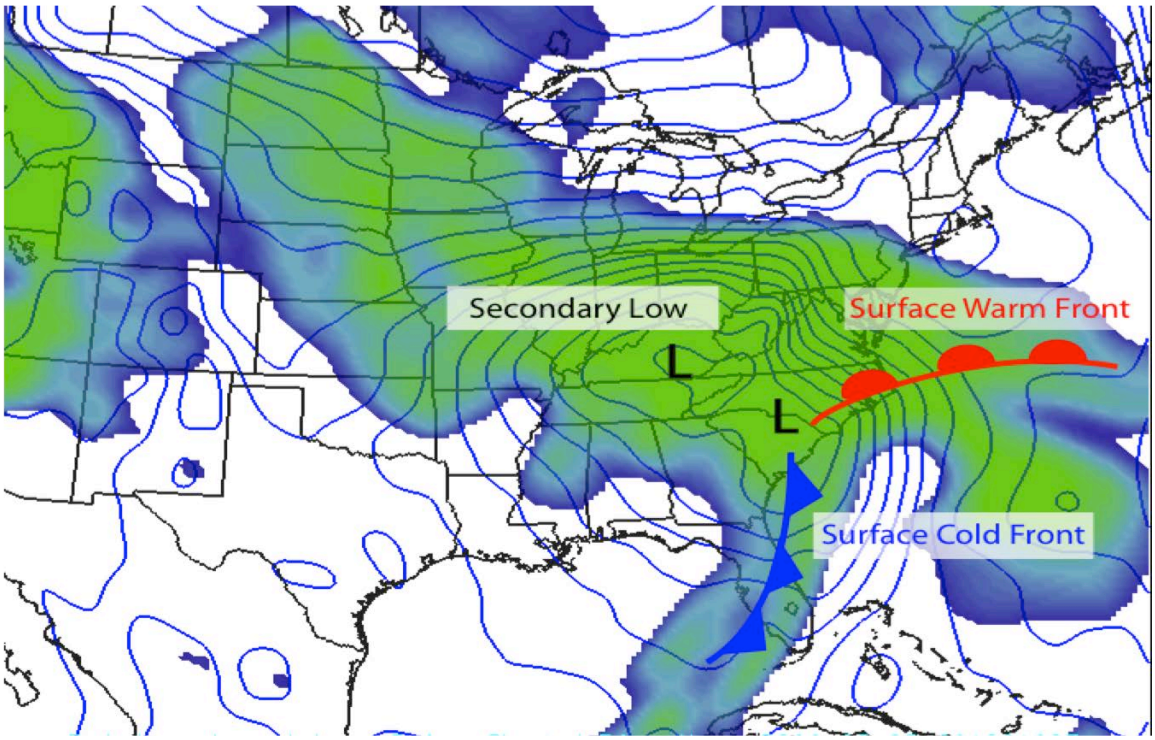

Figure 4.23. A plot the horizontal frontal features on top of the RUC 00-hr MSLP (contours) and 700 mb RH (shading >50%) from 6 February 2010 at 0000 UTC. An interesting feature of this IOP is the secondary low in the form of an Alberta Clipper system that impacted the winds at upper levels in IOP 17.

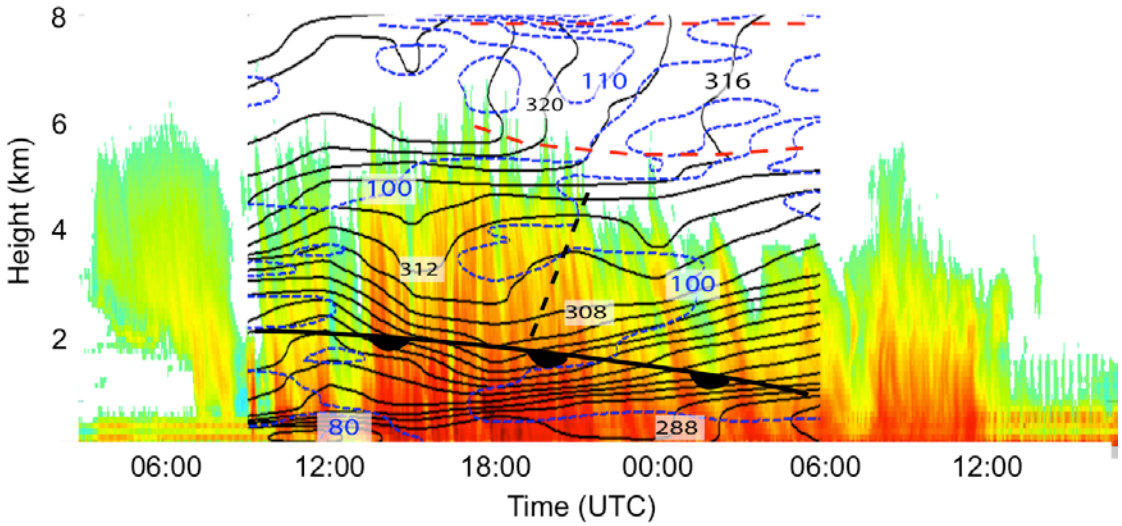

Figure 4.24. A plot of SNR, Θ_{ei} and RH_i, analysis of the vertical frontal structure, and evaluation of potential instability within this cyclone from 1600 UTC on 5 February to 0600 UTC on 6 February. The bottom red dashed line is the level where Θ_{ei} begins to alternate between slightly unstable to neutral with height., and the top red dashed line is the level where the original Θ_{ei} at the base of the unstable layer again appears.

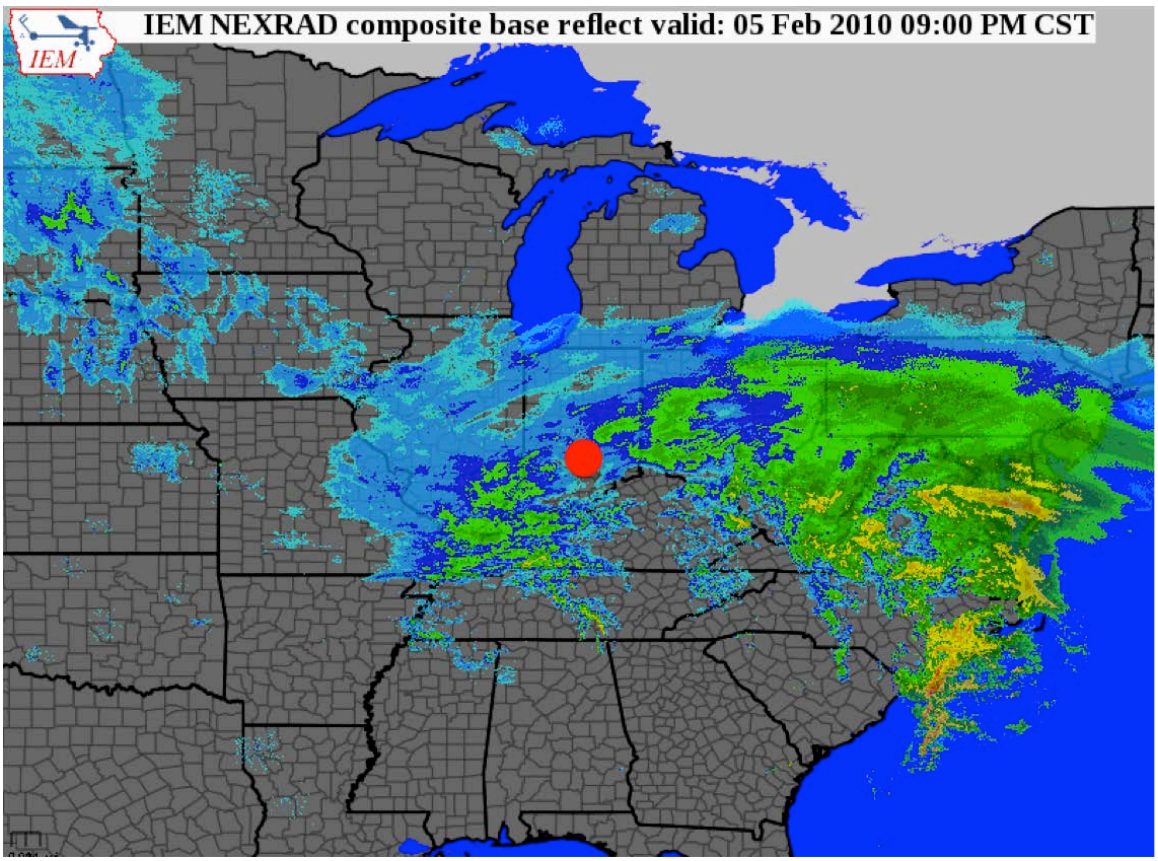

Figure 4.25. A national radar composite from 6 February 2010 at 0300 UTC. At this point in IOP 17, potential instability was indicated in the thermodynamic data in the wrap-around region, seen in Fig. 4.24. The profiler site, denoted by the red circle, is located on the south side of the comma-head region at this time.

Chapter 5: Conclusions

The purpose of this study was to determine if the area on the southern side of the comma-head region of continental winter cyclonic storms is associated with potential instability and upright convection. High-resolution radar and rawinsonde data were utilized in five separate case studies from the PLOWS field campaign to reveal that potential instability is indeed present in the northern extent of the cyclone and accompanied by convection. No two cyclones are the same, and this was demonstrated in this study by the vast differences that were seen between each cyclone. The cyclones in this study had varying frontal structures, origins, strengths, and upper level forcing, but they all had potential instability present. Based on these analyses, the moist/dry interface on the south side of the wrap-around region of wintertime continental cyclones is characterized by deep convective cells that have heights reaching the tropopause in many cases.

The data collected by the PLOWS field campaign and the subsequent analysis has led to an increased understanding of convective snowfall. The high-resolution view of winter storms that has been provided by the remote sensing instrumentation used during PLOWS can guide forecasters to correct their forecasts in the short-term and provide better nowcasting abilities. Using the knowledge that convective precipitation is common along the southern edge of the comma-head precipitation, forecasters can better predict the likelihood of the heavy snowfall events that impact millions of Americans each year.

Chapter 6: Bibliography

Bennetts, D. A., and B. J. Hoskins, 1979: Conditional symmetric instability – a possible explanation for frontal rainbands. Quart. J. Roy. Meteor. Soc., 105, 945-962.

Bluestein, H. B., 1993: Synoptic-Dynamic Meteorology in Midlatitudes. Vol. 2, Observations and Theory of Weather Systems. Oxford University Press, 594.

Douglas et al., 1957: Pattern in the Vertical of Snow Generation. J. of Meteorology, 14.2, 95-114.

Emanuel, K. A., 1983: The lagrangian parcel dynamics of moist symmetric instability. J. Atmos. Sci., 40, 2368-2376.

Langleben, M.P., 1956: The Plan Pattern of Snow Echoes at the Generating Level. J. of Meteorology, 13, 554-560.

Marshall, J.S., 1953: Precipitation trajectories and patterns. J. Atmos. Sci., 10, 25–29.

Martin, J. E., 1998b: The structure and evolution of a continental winter cyclone. Part II: Frontal forcing of an extreme snow event. Mon Wea. Rev., 126, 329-348.

Nicosia, D. J., and R. H. Grumm, 1999: Mesoscale band formation in three major northeastern United States snowstorms. Wea. Forecasting, 14, 346-368.

Novak et al., 2008: High-Resolution Observations and Model Simulations of the Life Cycle of an Intense Mesoscale Snowband over the Northeastern United States. Mon. Wea. Rev., 136, 1433-1456.

Novak et al., 2009: The Role of Moist Processes in the Formation and Evolution of Mesoscale Snowbands within the Comma Head of Northeast U.S. Cyclones. Mon. Wea. Rev., 137, 2662-2686.

Persson, P. O. G., and T. T. Warner, 1995: The nonlinear evolution of idealized, unforced, conditional symmetric instability: a numerical study. J. Atmos. Sci., 52, 3449-3474.

Rauber et al., 2012b: In Publication.

Reed, R. J., 1955: A Study of a Characteristic Type of Upper-Level Frontogenesis. J. of Meteorology, 12, 226-237.

Reed, R. J. and Sanders, F., 1953: An Investigation of the Development of a Mid-Tropospheric Frontal Zone and Its Associated Vorticity Field. J. of Meteorology, 10, 338-349.

Wexler, R., 1955: Radar analysis of precipitation streamers observed 25 February 1954. J. Atmos. Sci., 12, 391–393.

Wexler, R., and D. Atlas, 1959: Precipitation generating cells. J. Atmos. Sci., 16, 327–332.

Wiesmueller, J.L., and S.M. Zubrick, 1998: Evaluation and Application of Conditional Symmetric Instability, Equivalent Potential Vorticity, and Frontogenetic Forcing in an Operational Forecast Environment. Wea. Forecasting, 13, 84–101.